iScience

CellPress
OPEN ACCESS

Review

# Ultrafast Fiber Lasers: An Expanding Versatile Toolbox

Guoqing Chang[1,2,*] and Zhiyi Wei[1,2,3,*]

**Ultrafast fiber lasers have gained rapid advances in last decades for their intrinsic merits such as potential of all-fiber format, excellent beam quality, superior power scalability, and high single-pass gain, which opened widespread applications in high-field science, laser machining, precision metrology, optical communication, microscopy and spectroscopy, and modern ophthalmology, to name a few. Performance of an ultrafast fiber laser is well defined by the laser parameters including repetition rate, spectral bandwidth, pulse duration, pulse energy, wavelength tuning range, and average power. During past years, these parameters have been pushed to an unprecedented level. In this paper, we review these enabling technologies and explicitly show that the nonlinear interaction between ultrafast pulses and optical fibers plays the essential role. As a result of rapid development in both active and passive fibers, the toolbox of ultrafast fiber lasers will continue to expand and provide solutions to scientific and industrial problems.**

## INTRODUCTION

This year—2020—marks the 60$^{th}$ anniversary of the invention of laser. When Theodore Maiman invented laser in 1960, it was widely considered a "solution looking for a problem (Townes, 2002)." The past six decades have seen emergence of many types of lasers, which are grouped into different categories in terms of gain materials (e.g., gas, liquid, semiconductor, solid-state, fiber), pumping schemes (e.g., electrical pumping or optical pumping), cavity configuration (e.g., linear cavity or ring cavity), operation state (e.g., CW or pulsed), etc. As one subcategory, pulsed fiber lasers dated back to 1983 when partial mode-locking was first observed in a Nd-doped fiber laser (Dzhibladze et al., 1983). Several years later, improved mode-locking in Nd-doped fiber lasers produced picosecond or even femtosecond pulses (Fermann et al., 1990b; Wigley et al., 1990). However, research in ultrafast Nd-doped fiber lasers gradually diminished owing to the development of other active fibers with advantageous properties. These superior ultrafast fiber lasers work at three wavelength ranges; that is, ultrafast Yb-fiber lasers at ~1.03 μm, ultrafast Er-fiber lasers at ~1.55 μm, and ultrafast Tm-fiber or Ho-fiber lasers at ~2 μm. Figure 1 illustrates the number of publications as a function of year for these ultrafast lasers and indicates an exponential growth in last two decades. The figure discloses an interesting trend: the remarkable development of ultrafast Er-fiber lasers—spurred by optical communication booming in 1990s—was eventually overtaken by ultrafast Yb-fiber lasers in 2009; in the same year, ultrafast Tm-fiber/Ho-fiber lasers started to advance at a rapid pace.

The advances in ultrafast fiber lasers have been well documented in the last decade by many excellent review papers (Brida et al., 2014; Fermann and Hartl, 2009, 2013; Galvanauskas, 2001; Jackson, 2012; Jauregui et al., 2013; Limpert et al., 2006, 2007, 2011, 2014; Nilsson and Payne, 2011; Richardson et al., 2010; Shi et al., 2014; Tunnermann et al., 2005, 2010; Xu and Wise, 2013; Zervas, 2014; Zervas and Codemard, 2014; Nilsson et al., 2003), most of which focus on energy/power scalability of ultrafast Yb-fiber lasers. Indeed, laser parameters (e.g., repetition rate, spectral bandwidth, pulse duration, pulse energy, wavelength tuning range, average power) define the performance of an ultrafast laser. The last decade has witnessed a continuous expansion of the parameter space in which ultrafast fiber lasers can operate. In this paper, we review the enabling technologies that has continued to push the boundaries of the laser parameters. This review is structured as follows. In the next section, we present a brief introduction to nonlinear fiber optics that deals with propagation of femtosecond pulses inside optical fibers followed by a discussion of ultrafast fiber oscillators/amplifiers. We then continue to review the last-decade progress in enlarging the coverage of laser parameters—such as repetition rate, pulse energy, average power, and center wavelength—of ultrafast fiber laser systems. The last section presents conclusion and outlook.

[1]Beijing National Laboratory for Condensed Matter Physics, Institute of Physics, Chinese Academy of Sciences, Beijing 100190, China

[2]School of Physical Sciences, University of Chinese Academy of Sciences, Beijing 100190, China

[3]Songshan Lake Materials Laboratory, Dongguan, Guangdong 523808, China

*Correspondence: guoqing.chang@iphy.ac.cn (G.C.), zywei@iphy.ac.cn (Z.W.)

https://doi.org/10.1016/j.isci.2020.101101

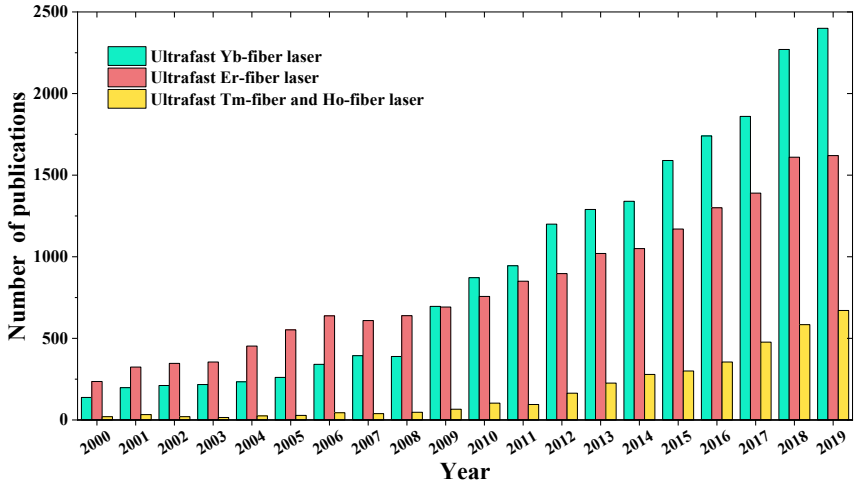


**Figure 1. Number of Publications Versus Year from Google Scholar**

Key search words: ultrafast ytterbium fiber laser, ultrafast erbium fiber laser, ultrafast thulium fiber laser, and ultrafast holmium fiber laser.

## NONLINEAR PHENOMENA ASSOCIATED WITH PROPAGATION OF ULTRASHORT PULSES IN ACTIVE AND PASSIVE FIBERS

An ultrafast fiber laser system undoubtedly involves propagation of ultrashort pulses inside passive fibers and active fibers. Owing to long interaction length, tight confinement of light inside fiber core area, and high peak power from an ultrashort pulse, such propagation gives rise to various nonlinear phenomena. Understanding how an ultrafast fiber laser works and then improving its performance highly relies on the knowledge of nonlinear fiber optics, a field that explicitly investigates the nonlinear propagation of ultrashort optical pulses inside fibers (Agrawal, 2006). The propagation can be accurately described by the following generalized nonlinear Schrödinger equation (GNLSE) that takes into account both linear and nonlinear effects:

$$\frac{\partial A}{\partial z}+\left(\sum_{n\geq 2}\beta_n\frac{i^{n-1}}{n!}\frac{\partial^n}{\partial T^n}\right)A=i\gamma\left(1+\frac{i}{w_0}\frac{\partial}{\partial T}\right)\left(A(z,T)\int_{-\infty}^{+\infty}R(t')|A(z,T-t')|^2dt'\right)+\frac{g}{2}A \quad \text{(Equation 1)}$$

where A(z, T) describes the slowly varying amplitude envelope of the pulse. $\beta_n$ represents the $n^{th}$-order fiber group-velocity dispersion (GVD). $\gamma$ is the nonlinear parameter defined as $\gamma = \omega_0 n_2/(cA_{eff})$. $\omega_0$ is the center frequency, $n_2$ the nonlinear-index coefficient of the fiber material, $c$the light speed in vacuum, and $A_{eff}$ the mode-field area (MFA). R(t) includes both the instantaneous electronic and delayed molecular responses (i.e., Raman response) and is normally given by:

$$R(t) = (1-f_R)\delta(t)+f_R h_R(t) \quad \text{(Equation 2)}$$

where $f_R$ represents the fractional contribution of the Raman response to nonlinear polarization $P_{NL}$. $h_R(t)$ denotes the Raman response function. The last term on the right-hand side of Equation 1 accounts for optical fiber amplification; that is, g > 0 (g = 0) corresponds to pulse propagation inside an active (passive) optical fiber.

As the essential equation in the field of nonlinear fiber optics, GNLSE describes complicated nonlinear pulse evolution (Agrawal, 2006) and can be numerically solved by the split-step Fourier method. Nevertheless, to clarify the physics behind a specific nonlinear phenomenon, reduced forms of GNLSE are usually adopted for analytical analysis. Below is a list of frequently encountered examples in the ultrafast fiber laser technology.

### Soliton Formation

If only the second-order dispersion and self-phase modulation (SPM) are considered, Equation 1 can be simplified to the standard NLSE

$$\frac{\partial A}{\partial z}+i\frac{\beta_2}{2}\frac{\partial^2 A}{\partial T^2}=i\gamma|A|^2A \quad \text{(Equation 3)}$$

For a pulse propagating in a fiber with positive GVD (i.e., $\beta_2 > 0$), both SPM and GVD exert positive chirp to the pulse. For enough propagation distance, optical wave breaking occurs that manifests as rapid oscillations appearing near pulses edges (Anderson et al., 1992; Tomlinson et al., 1985). In contrast, negative GVD (i.e., $\beta_2 < 0$) allows soliton formation. Owing to a balance between dispersion and nonlinearity, a fundamental soliton pulse maintains its profile during the propagation inside a passive fiber. The pulse energy needs to satisfy the well-known soliton area theorem:

$$E = \frac{1}{\gamma}\frac{|\beta_2|}{T_0^2} = \frac{cA_{eff}|\beta_2|}{\omega_0 n_2 T_0^2} \quad \text{(Equation 4)}$$

where $T_0$ is connected to the full-width-at-half-maximum (FWHM) of the pulse by $T_0 \sim T_{FWHM}/1.763$ (Agrawal, 2006). Equation 3 accommodates higher-order solitons as well. Unlike a fundamental soliton, higher-order solitons evolve periodically in both the temporal domain and the spectral domain during the propagation. Soliton pulses are stable if only SPM and negative GVD exist. However, as they propagate inside an optical fiber, other effects as included in the GNLSE are inevitable and, under certain circumstances, may be treated as perturbation sources to a soliton. In the following two sections, we briefly discuss two important phenomena related with soliton perturbation.

### Dispersive Wave Generation

If the optical pulse has a broad optical spectrum or its center wavelength is close to the zero-dispersion wavelength of the fiber, higher-order dispersion terms need to be included:

$$\frac{\partial A}{\partial z} + \left(\sum_{n\geq 2}\beta_n \frac{i^{n-1}}{n!}\frac{\partial^n}{\partial T^n}\right)A = i\gamma|A|^2 A \quad \text{(Equation 5)}$$

These higher-order dispersions perturb a fundamental soliton and cause radiation of an optical pulse centered at a new frequency given by the following phase-matching condition:

$$\sum_{n\geq 2}\frac{(\omega-\omega_0)^n}{n!}\beta_n(\omega_0) - \frac{\gamma P_0}{2} = 0 \quad \text{(Equation 6)}$$

This phenomenon—widely known as dispersive wave generation (or non-solitonic radiation, fiber-optic Cherenkov radiation)—was first theoretically studied in 1986 (Wai et al., 1986). With the advent of photonic-crystal fibers (PCFs) that allow one to flexibly engineer fiber dispersion, dispersive wave generation attracted intensive research attention under the context of supercontinuum generation (Austin et al., 2006; Cristiani et al., 2004) and later became a useful method for nonlinear wavelength conversion (Chang et al., 2010, 2011). Detailed analysis shows that the sign of the third-order dispersion (TOD, i.e., $\beta_3$) determines whether the center wavelength of the dispersive wave pulse is downshifted or upshifted with respect to the soliton center wavelength (Akhmediev and Karlsson, 1995; Karpman, 1993). Positive (negative) TOD produces dispersive wave centered at a shorter (longer) wavelength compared with the soliton.

### Soliton Self-Frequency Shift

In Equation 3, only the instantaneous electronic response of fused silica is included, which gives rise to the SPM effect. Indeed, delayed molecular responses (i.e., Raman response)—represented by the second term in Equation 2—leads to intra-pulse Raman scattering such that the center wavelength of a soliton continuously shifts toward longer wavelength. This phenomenon is known as soliton self-frequency shift (SSFS) (Gordon, 1986; Mitschke and Mollenauer, 1986). Similar as dispersive wave generation, SSFS has been fully explored for investigating supercontinuum generation in PCFs and governs the extension of the spectrum toward the longer wavelength side (Husakou and Herrmann, 2001). In the time domain, SSFS generates wavelength-tunable transform-limited pulses (known as Raman soliton pulses) and the amount of wavelength shift can be readily adjusted by varying the input pulse energy. Together with the rapid development of fiber technology, SSFS constitutes a powerful method to produce wavelength-tunable femtosecond pulses.

### Parabolic Similariton Asymptotically Developed in Fiber Amplifier

As an optical pulse propagates inside an active fiber (e.g., Yb-doped fiber amplifier), Equation 3 should be modified to take into account the gain effect, leading to the following equation:

$$\frac{\partial A}{\partial z} + i\frac{\beta_2}{2}\frac{\partial^2 A}{\partial T^2} = i\gamma|A|^2 A + \frac{g}{2}A \qquad \text{(Equation 7)}$$

If the fiber exhibits positive GVD ($\beta_2 > 0$), the interplay among dispersion, SPM, and gain renders an input pulse of arbitrary shape evolving asymptotically into an amplified, linearly chirped pulse with a parabolic intensity profile (Boscolo et al., 2002; Kruglov et al., 2000, 2002). During further propagation, this parabolic pulse evolves in a self-similar manner such that the temporal profile and the chirp rate remain unchanged while the pulse duration, peak power, and spectral bandwidth increase exponentially with the distance. Such an optical pulse is referred to as similariton or, more specifically, parabolic similariton. First experimentally observed in an Yb-fiber amplifier (Fermann et al., 2000), parabolic similariton was soon found in Raman fiber amplifier (Finot et al., 2003), fiber oscillators (Ilday et al., 2004; Oktem et al., 2010), and dispersion-decreasing fibers (Finot et al., 2007; Hirooka and Nakazawa, 2004). Indeed, similariton is a universal phenomenon and can emerge from optical beam propagation (parabolic spatial similariton) (Chang et al., 2006) or an incoherent nonlinear system (incoherent similariton) (Chang et al., 2005). Detailed progress in research on similariton was well documented in review papers (Chong et al., 2015; Dudley et al., 2007; Finot et al., 2009).

## MAIN BUILDING BLOCKS OF ULTRAFAST FIBER LASER SYSTEMS

Most ultrafast fiber lasers in practical use are configured in a master-oscillator-power-amplifier (MOPA) architecture; that is, an ultrafast fiber oscillator provides stable pulses, which are then amplified by subsequent fiber amplifiers to boost the average power and pulse energy. In the following we briefly discuss ultrafast fiber oscillator and amplifier, respectively.

### Ultrafast Fiber Oscillator

In a MOPA system, the fiber oscillator is passively mode-locked at the fundamental repetition rate. Mode-locking for producing femtosecond pulses is achieved through saturable absorption of the intra-cavity circulating pulse. Such saturable absorption may be implemented by a non-fiber device, known as saturable absorber, which involves direct material absorption. During the past decade, many ultrafast fiber oscillators—especially Er-fiber oscillators—were mode-locked by a saturable absorber made of novel materials, such as carbon nanotube (Set et al., 2004), graphene (Bao et al., 2009), perovskite (Hong et al., 2018), transition metal dichalcogenides (Woodward and Kelleher, 2015), and topological materials (Liu et al., 2016b), to name a few. Nevertheless, semiconductor saturable absorber mirrors (SESAM)—an old technology dated to 1990—are widely believed to still outperform the above-mentioned devices (Keller et al., 1990, 1996; Okhotnikov et al., 2004).

Besides saturable absorbers made from real materials that involve light absorption, an alternative is to employ fiber-optic nonlinear effects followed by a device to achieve effective saturable absorption. For example, propagation of an elliptically polarized pulse inside an optical fiber may experience nonlinear polarization evolution (NPE); that is, different parts of the pulse (e.g., peak versus wing) exhibit different polarization states. Consequently, a properly aligned polarizer allows more transmission of the peak than the wing and the transmitted pulse becomes shorter. The NPE together with the polarizer thus forms an artificial saturable absorber to mode-lock fiber lasers (Fermann et al., 1993); the resulting lasers are often called NPE fiber lasers. Another type of artificial saturable absorber is configured as a fiber loop connected with the laser cavity by a fiber coupler; typical implementation includes nonlinear-optical loop mirror (Doran and Wood, 1988) and nonlinear amplifying loop mirror (NALM) (Fermann et al., 1990a; Hänsel et al., 2017; Jiang et al., 2016). The intra-cavity pulse is split into two replicas by the coupler before entering the fiber loop such that one replica propagates in the clockwise direction and the other in the counter-clockwise direction. After traveling one round trip in the loop, these two pulses accumulate different nonlinear phase shift and interfere at the coupler before they return to the laser cavity. Figure 2 shows an Yb-doped fiber oscillator constructing from all polarization-maintaining (PM) fibers mode-locked by NALM (Yu et al., 2018b). Two optical loops (main loop on the left and NALM loop on the right) constructed from PM fiber components are connected by a 2 × 2 coupler to form a figure-of-eight cavity. The main loop provides cavity for oscillation, whereas the NALM loop behaves as an artificial saturable absorber that enables mode-locking. This all-fiber oscillator can emit 6-MHz, 93-fs pulses with 10 nJ pulse energy after external compression (Yu et al., 2018b).

Recently, a new type of fiber oscillator, dubbed as Mymeshev oscillator, emerged and quickly attracted intensive research interest (Liu et al., 2017b, 2019; Regelskis et al., 2015; Sidorenko et al., 2018). In a

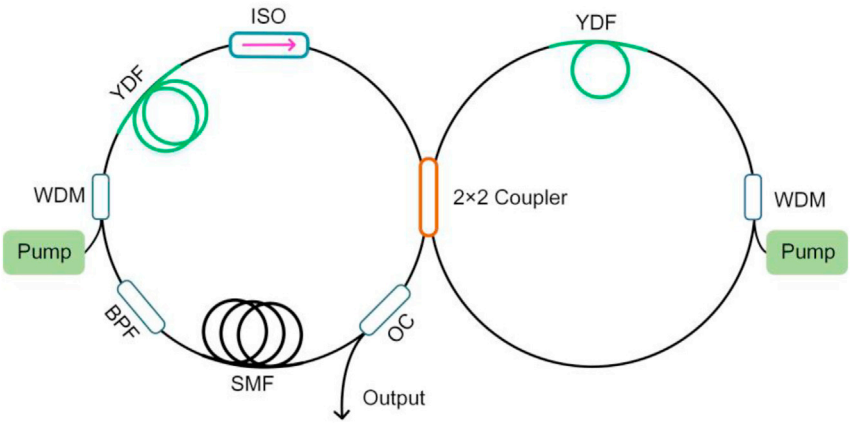


**Figure 2. Experimental Setup of a Mode-Locked Yb-Doped All-PM-Fiber Oscillator Mode-Locked by NALM**
The left loop constitutes the laser main cavity and the right one is an NALM. YDF, Yb-doped fiber; WDM, wavelength division multiplexer; ISO, isolator; BPF, bandpass filter; OC, output coupler.

Mymeshev oscillator, fiber-optic nonlinearity that causes substantial spectral broadening and two bandpass optical filters that center at different wavelengths work jointly as two cascaded Mymeshev regenerators (Regelskis et al., 2015). Only a suitable ultrashort pulse can circulate inside the laser cavity; a CW background (or weak pulse) cannot exist because two bandpass filters have no overlap in transmission. These cascaded Mymeshev regenerators are equivalent to an artificial saturable absorber with 100% modulation depth (Liu et al., 2017b).

Passive mode-locking ensures that the intra-cavity pulse can circulate stably in the fiber oscillator cavity. However, the evolution of the intra-cavity pulse in one round trip highly depends on the cavity dispersion map. In other words, managing the cavity dispersion can control the operation state of a fiber oscillator. Depending on the amount of net cavity dispersion and its sign, the circulating pulse inside the cavity ranges from sub-ps to >10 ps in duration corresponding to different mode-locking regimes (e.g., soliton, stretched pulse, similariton, and dissipative soliton) (Chong et al., 2008; Wise et al., 2008). For Yb-fiber laser at ~1.03 μm, conventional fibers exhibit positive GVD. To manage the cavity dispersion, negative GVD is introduced by grating pairs (Treacy, 1969), PCFs (Birks et al., 1999), or chirped fiber Bragg gratings (CFBGs) (Hill et al., 1994). For Er-fiber laser at ~1.55 μm, many types of solid-core fibers—such as dispersion-shifted fibers, dispersion compensation fibers, dispersion decreasing fibers—are developed to engineer the fiber dispersion. At this wavelength, both passive and active PM fibers with either positive or negative GVD are commercially available.

## Ultrafast Fiber Amplifier

Although much research effort has been devoted in power/energy scaling a fiber oscillator, a conventional wisdom toward producing high-power/energy femtosecond pulses is to rely on a MOPA system. In a MOPA system, the master oscillator only needs to provide low-power/energy pulses and thus can be carefully engineered to achieve low noise, high compactness, and extreme robustness. The weak seeding pulses are then amplified in subsequent fiber amplifiers by orders of magnitude in pulse energy or average power. In most cases, the performance of a fiber laser system strongly depends on the amount of nonlinear phase shift accumulated by the pulse. For a fixed nonlinear phase shift, increasing the MFA allows higher pulse peak-power inside the gain fiber. To date, most fiber amplifiers that output >1 W average power are constructed from double-clad large-mode-area (LMA) fibers. The double-clad structure—first demonstrated in 1988—has become the standard technique that allows pumping an active fiber using high-power multimode laser diodes (Snitzer et al., 1988). In the last two decades, many groups proposed and demonstrated double-clad active fibers with increased core MFA, such as chirally coupled core fibers (Liu et al., 2007), leakage channel fibers (Dong et al., 2009), and rod-type fibers (Limpert et al., 2005). Recently developed rod-type large-pitch fibers (LPFs) delocalize the higher-order modes resulting in their poor overlapping with the doped core region; as a result, the differential gain between the fundamental mode and higher-order modes guarantees robust single-mode operation of amplifiers constructed from rod-type LPF amplifiers (Stutzki et al., 2011). The mode-field diameter (MFD) of an Yb-doped rod-type LPF can

exceed 100 μm, corresponding to an MFA 100 times larger than that offered by conventional single-mode fibers (Limpert et al., 2012).

## ENLARGE THE PARAMETER SPACE TO EXPAND FIBER LASER TOOLBOX

An ultrafast fiber laser system is well characterized by several measurable parameters such as repetition rate, pulse energy, pulse duration, peak power, average power, and center wavelength. In practice, a specific application demands optimization of a subset of these parameters. Indeed, optimizing some parameters unavoidably compromises other parameters in reality owing to technical limitations. In this section we review the typical parameter space of ultrafast fiber laser systems.

### Repetition Rate

Scientific and industrial applications may demand femtosecond pulses with the repetition rate ranging from 1 kHz to >10 GHz. The cavity length determines the repetition rate of a fundamentally mode-locked ultrafast fiber oscillator. Most fiber oscillators include several-meter-long optical fibers and the typical repetition rate is tens of MHz. Adding more passive fibers into the cavity can lower down the repetition rate. However, reducing the repetition rate below 1 MHz from a ring-cavity oscillator corresponds to a cavity of about 200 m in length. Such a long cavity suffers from two drawbacks: (1) the oscillator is vulnerable to ambient disturbances, which may destroy mode-locking and (2) the output pulse develops nonlinear and gigantic chirp making the pulse hard to compress. In practical implementation, ultrashort pulses with a repetition rate below 10 MHz are derived from an ultrafast fiber laser system via pulse picking enabled by an acousto-optic pulse picker.

Mode-locking of a fiber laser at a repetition rate above 200 MHz is challenging as well. Especially as the repetition rate exceeds 1 GHz, the cavity fiber is less than 10 cm in length and therefore the active fiber must be highly doped to provide enough gain. Table 1 lists representative ultrafast Yb-doped and Er-doped fiber oscillators fundamentally mode-locked with the repetition rate beyond 150 MHz (Byun et al., 2010; Chen et al., 2007, 2012b; Cheng et al., 2017, 2018; Du et al., 2017; Huang et al., 2017; Ilday et al., 2005; Li et al., 2013, 2014a, 2014b, 2015; Liu et al., 2018; Ma et al., 2010; Martinez and Yamashita, 2011, 2012; Song et al., 2019a, 2019b; Wang et al., 2011, 2019; Wu et al., 2015a; Xing et al., 2015; Yang et al., 2012; Zhang et al., 2016).

Limited by the available power from single-mode pump diodes, increased repetition rate is usually accompanied by reduced pulse energy. For GHz ultrafast fiber lasers, the pulse energy may be as low as sub-pJ (Martinez and Yamashita, 2011, 2012). Because of reduced pulse energy and short fiber length, the intracavity pulse accumulates less nonlinear phase shift in each round trip and the associated nonlinear pulse shaping is weakened, leading to narrower optical spectrum and longer pulse. Figure 3 illustrates the pulse duration as a function of repetition rate for ultrafast Yb-doped and Er-doped fiber lasers; each type of fiber lasers can be configured in linear cavity or ring cavity. In general, given the same type of active fibers (Yb-doped versus Er-doped), linear-cavity configuration results in higher repetition rate than can be achieved from ring-cavity configuration.

It is noteworthy that highly doped Yb-fibers exhibit positive GVD, which necessitates dispersion compensation for the oscillator cavity in order to produce femtosecond pulses. For example, we demonstrated a 3-GHz fiber oscillator using 1-cm, heavily Yb-doped phosphate glass fiber as the gain medium (Chen et al., 2012b). To compensate for the positive GVD, the output coupler was specially designed with custom coating structures that provides $-1{,}300\ fs^2$ group-delay dispersion at 1.03 μm making the net cavity dispersion slightly negative. Such a compact Yb-fiber oscillator produces 3-GHz pulses with the pulse duration as short as 206 fs (Chen et al., 2012b). Recently, Yb-fiber oscillators with >5-GHz repetition rate are demonstrated (Cheng et al., 2017, 2018; Liu et al., 2018; Wang et al., 2019); without dispersion compensation, these oscillators emit picosecond pulses. In contrast, highly doped Er-fibers have negative GVD and the resulting oscillators can operate at soliton mode-locking regime without requirement of dispersion compensation. To date, the highest repetition rate of a fundamentally mode-locked Er-fiber oscillator is 19.45 GHz and the output pulse has a duration of 790 fs (Martinez and Yamashita, 2011).

Some applications (e.g., all-optical sampling, precision metrology) desire that the repetition rate of an ultrafast laser can be tuned in a range exceeding ±1%. In the context of frequency comb applications, the repetition rate of a fiber oscillator determines the frequency spacing between two adjacent comb lines. In this scenario, tuning the repetition rate can precisely vary the comb spacing. Since the repetition rate is determined by the round-trip

| | Cavity | λ (nm) | $E_p$ (pJ) | $\tau_p$ (fs) | $f_{rep}$ (GHz) | Reference |
|---|---|---|---|---|---|---|
| YDF | Linear (SA) | 1,025 | 17.7 | 206 | 3 | (Chen et al., 2012b) |
| | | 1,059 | 8–16 | 2,600 | 5 | (Cheng et al., 2017) |
| | | 1,041 | 19 | 3,400 | 3 | (Cheng et al., 2018) |
| | | 1,060 | NA | 3,200 | 3.1 | (Wang et al., 2019) |
| | | 1,050 | NA | 3,200 | 7.0 | (Wang et al., 2019) |
| | | 1,047 | NA | 1,900 | 12.5 | (Wang et al., 2019) |
| | Ring (NPE) | 1,035 | 150 | 70* | 0.162 | (Ilday et al., 2005) |
| | | 1,030 | 320 | 156 | 0.503 | (Wang et al., 2011) |
| | | 1,030 | 920 | 502 | 0.605 | (Yang et al., 2012) |
| | | 1,035 | 280 | 68* | 0.75 | (Li et al., 2013) |
| | | 1,020 | 731 | 98* | 0.616 | (Li et al., 2014a) |
| | | 1,030 | 600 | 64* | 1.0 | (Li et al., 2015) |
| | | 1,027 | 214 | 215 | 0.7 | (Liu et al., 2018) |
| EDF | Linear (SA) | 1,573 | 283 | 187 | 0.967 | (Byun et al., 2010) |
| | | 1,600 | 0.15 | 680 | 4.24 | (Martinez and Yamashita, 2011) |
| | | 1,560 | 0.26 | 940 | 9.64 | (Martinez and Yamashita, 2011) |
| | | 1,563 | 0.32 | 790 | 19.45 | (Martinez and Yamashita, 2011) |
| | | 1,562 | 0.16 | 865 | 9.67 | (Martinez and Yamashita, 2012) |
| | | 1,556 | 13 | 935 | 0.463 | (Wu et al., 2015a) |
| | | 1,558 | 7.3 | 379 | 1.0 | (Huang et al., 2017) |
| | | 1,588 | NA | 639 | 3.2 | (Cheng et al., 2018) |
| | | 1,558 | 160.5 | 244* | 2.68 | (Song et al., 2019b) |
| | | 1,553 | 5.34 | 550 | 1.03 | (Song et al., 2019a) |
| | Ring (NPE) | 1,565 | 154.6 | 167 | 0.194 | (Chen et al., 2007) |
| | | 1,555 | 310 | 37.4* | 0.225 | (Ma et al., 2010) |
| | | 1,553 | 420 | 56.5 | 0.202 | (Xing et al., 2015) |
| | | 1,560 | 174.1 | 180 | 0.517 | (Zhang et al., 2016) |
| | | 1,561 | 39 | 115 | 0.354 | (Du et al., 2017) |
| | NPE + SA | 1,552 | 310 | 41.9* | 0.212 | (Li et al., 2014b) |

**Table 1. The Evolution of High-Repetition-Rate Ultrafast Er/Yb Fiber Laser**

YDF, Yb-doped fiber; EDF, Er-doped fiber; SA, saturable absorber; NPE, nonlinear polarization evolution. Pulse duration marked with * indicates that the pulses are externally compressed or the duration corresponds to calculated transform-limited pulse.

time of the intra-cavity circulating pulse, tuning the repetition rate was normally achieved by introducing a tunable optical delay line into the cavity of a passively mode-locked fiber oscillator (Hundertmark et al., 2004; Liu et al., 2010; Washburn et al., 2004; Wu et al., 2015b; Yang et al., 2016).

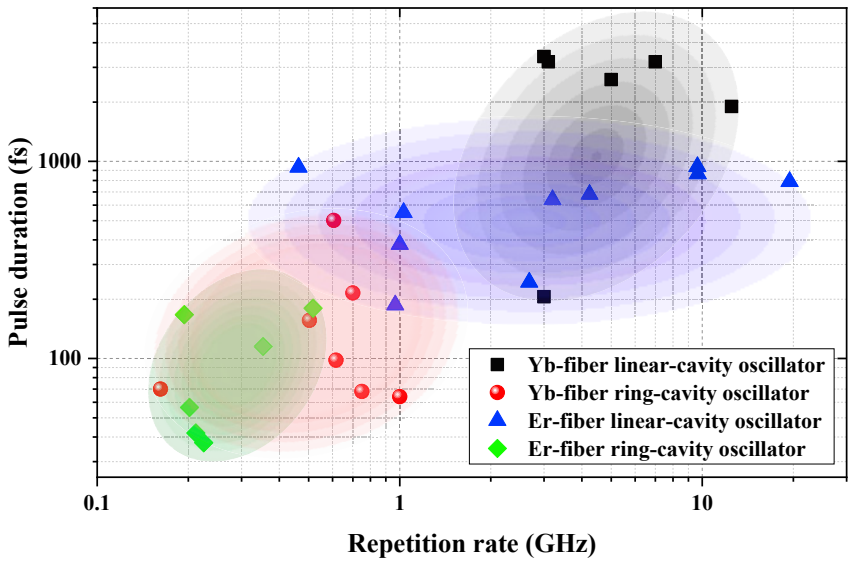


**Figure 3. Pulse Duration as a Function of Repetition Rate for Ultrafast Yb-Fiber and Er-Fiber Oscillators with the Repetition Rate Exceeding 150 MHz**

The results are grouped into four categories: (1) Yb-fiber linear-cavity oscillators (black squares), (2) Yb-fiber ring-cavity oscillators (red circles), (3) Er-fiber linear cavity oscillators (blue triangles), and (4) Er-fiber ring-cavity oscillator (green diamonds).

In recent years, dual-comb spectroscopy has emerged as a powerful spectroscopic technology, which holds promise for many important applications (Coddington et al., 2016; Ideguchi et al., 2014; Millot et al., 2016; Suh et al., 2016; Villares et al., 2014; Yu et al., 2018a). This technology requires two frequency combs with different comb spacing, which are normally achieved based on two ultrafast oscillators mode-locked at different repetition rates. A more attractive way to implement such a dual comb is to mode-lock a single fiber oscillator in a way such that it emits two pulse trains at different repetition rates (Mehravar et al., 2016; Zhao et al., 2016). As a result, the resulting two pulse trains can maintain mutual coherence. This type of ultrafast fiber oscillators are carefully designed such that two pulses circulate inside the oscillator cavity. To guarantee different round-trip times (and therefore different repetition rates), special efforts should be undertaken to ensure that these two intra-cavity pulses are different in polarization (Akosman and Sander, 2017; Deng et al., 2019; Guo et al., 2019; Nakajima et al., 2019), center wavelength (Chen et al., 2019; Guo et al., 2018; Hu et al., 2017, 2018; Jin et al., 2020; Li et al., 2018b; Liao et al., 2018; Mehravar et al., 2016; Nitta et al., 2018; Olson et al., 2018; Pawliszewska et al., 2020; Shi et al., 2018; Wang et al., 2016; Yun et al., 2012; Zhao et al., 2011, 2012a, 2016, 2019), or propagation path (Cui and Liu, 2013; Kayes et al., 2018; Mao et al., 2013). Table 2 summarizes the typical results of these dual-comb mode-locked fiber oscillators in terms of laser type, center wavelengths of the two pulse trains, repetition rate, and repetition-rate difference.

## Energy and Power Scaling

A fiber oscillator normally emits ultrashort pulses with nJ-level pulse energy, and the average power is below 100 mW. Further energy/power scaling relies on a MOPA system that involves amplifying ultrashort pulses in active fibers. The first ultrafast fiber amplifier—which was reported in 1989—was constructed from an erbium-doped fiber pumped by a diode laser (Nakazawa et al., 1989; Suzuki et al., 1989). Compared with Er-fiber MOPA system, Yb-fiber amplifiers feature much higher optical-to-optical conversion efficiency (~80%) and hence become the best fiber laser system capable of delivering high-energy and high-power femtosecond pulses (Paschotta et al., 1997). Amplification of ultrashort pulses has to deal with fiber-optic nonlinearities because excessive nonlinear phase shift may introduce complicated chirp to the amplified pulse, making it uncompressible. We divide amplification techniques into two main categories—linear amplification and nonlinear amplification—depending on whether the optical spectrum of the amplified pulses becomes much broader than the input spectrum.

| | Cavity | $\lambda_1$ (nm) | $\lambda_2$ (nm) | $f_{rep}$ (MHz) | $\Delta f$ (kHz) | Reference |
|---|---|---|---|---|---|---|
| EDF | Ring | 1,532.2 | 1,557.3 | 9.09 | 0.58 | (Zhao et al., 2011) |
| | | 1,532.4 | 1,556 | 15.75 | 0.466 | (Zhao et al., 2012a) |
| | | 1,550 | 1,562 | 7.68 | 889 | (Mao et al., 2013) |
| | | 1,560 | 1,560 | 7.05 | 4,480 | (Cui and Liu, 2013) |
| | | 1,533 | 1,544 | 52.74 | 1.25 | (Zhao et al., 2016) |
| | | 1,554.3 | 1,555.1 | 72.38 | 0.082 | (Mehravar et al., 2016) |
| | | 1,531.4 | 1,556.1 | 32.07 | 1.63 | (Hu et al., 2017) |
| | | 1,531.7 | 1,555.2 | 50.64 | 2.13 | (Shi et al., 2018) |
| | | 1,533 | 1,543 | 64.55 | 0.248 | (Hu et al., 2018) |
| | | 1,530 | 1,560 | 48.80 | 0.217 | (Nitta et al., 2018) |
| | | 1,559.4 | 1,559.6 | 20.9 | 0.009 | (Guo et al., 2018) |
| | | 1,570 | 1,581 | 40.52 | 0.93 | (Li et al., 2018b) |
| | | 1,554.5 | 1,565.3 | 24.83 | 0.633 | (Zhao et al., 2019) |
| | | 1,560 | 1,560 | 98.94 | 1.4 | (Guo et al., 2019) |
| | | 1,551.9 | 1,560 | 68.67 | 2.621 | (Chen et al., 2019) |
| | | 1,539.5 | 1,564.4 | 21.20 | 0.009 | (Nakajima et al., 2019) |
| | | 1,530 | 1,556 | 28.90 | 0.058 | (Jin et al., 2020) |
| | Figure-8 | 1,572 | 1,587 | 3.28 | NA | (Yun et al., 2012) |
| | Linear | 1,541 | 1,541 | 46.73 | 11.989 | (Deng et al., 2019) |
| TDF | Ring | 1,943.6 | 1,972 | 23.48 | 2.633 | (Wang et al., 2016) |
| | | 1,956.8 | 1,979.2 | 10.77 | 0.316 | (Wang et al., 2016) |
| | | 1,911 | 1,913 | 16.57 | 1.3 | (Kayes et al., 2018) |
| | | 1,917 | 1,981 | 71.88 | 3.27 | (Liao et al., 2018) |
| | | 1,870[a] | 1,870[a] | 60.78 | 0.229[a] | (Olson et al., 2018) |
| T/HDF | Linear | 1,975 | 1,975 | 67.62 | 0.51 | (Akosman and Sander, 2017) |
| HDF | Ring | 2,021 | 2,096 | 48.29[a] | 8[a] | (Pawliszewska et al., 2020) |

**Table 2. Dual-Comb Fiber Oscillators that Emit Two Pulse Trains at Different Repetition Rates**
EDF, Er-doped fiber; TDF, Tm-doped fiber; T/HDF, Tm/Ho-doped fiber; HDF, Ho-doped fiber.
[a]Minimum value.

### *Linear Amplification*

Chirped-pulse amplification (CPA)—the mature technique used in solid-state amplifiers—is a linear amplification technique, which was introduced in fiber amplifiers in 1993 (Stock et al., 1993) and soon adopted by most fiber amplifiers that produced pulses with >1 μJ pulse energy. A fiber CPA system typically includes (1) an ultrafast fiber oscillator providing weak seeding pulse, (2) a pulse stretcher that elongates the seeding pulse up to nanosecond level, (3) one- or multi-fiber amplifiers, and (4) a pulse compressor that dechirps the amplified pulse back to nearly transform-limited pulse duration. In the early demonstrations, Martinez-type diffraction-grating pair (Martinez, 1987) and Treacy-type grating pair (Treacy, 1969) are used as the stretcher and compressor, respectively. These grating pairs feature a large footprint and need precise alignment. These drawbacks are avoided by replacing diffraction gratings with chirped volume Bragg gratings (CVBGs) constructed from photo-thermo-refractive glass (Chang et al., 2009; Liao et al., 2007). Although CVBGs are compact, they are free-space devices

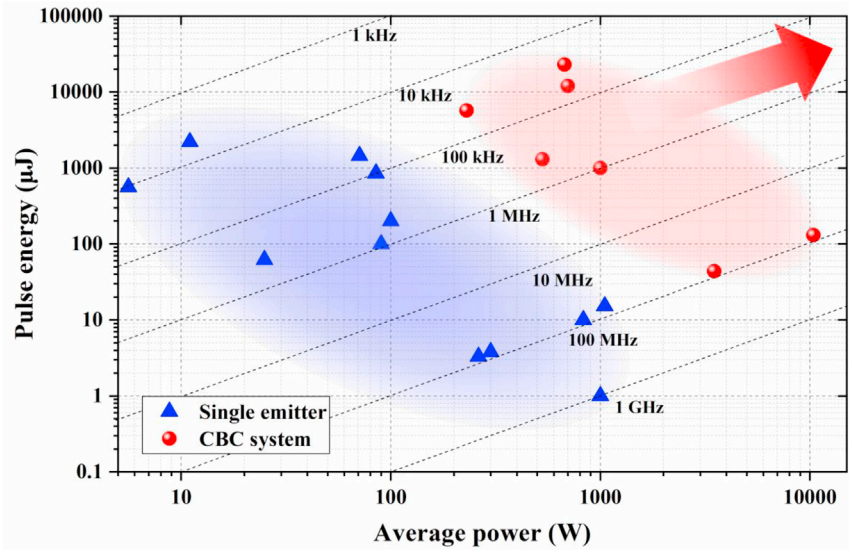


**Figure 4. Pulse Energy as a Function of Average Power for Yb-Fiber CPA Systems**
Triangles: single emitters; circles: CPA systems incorporating DPA and CBC. Dashed lines mark the repetition rate.

as well. To achieve a MOPA of all-fiber format, the stretcher is usually constructed from PM fibers or CFBGs that provide negative group-delay dispersion. To accommodate the amplified pulses with large pulse energy, hollow-core photonic-bandgap fibers were used as the compressor (de Matos et al., 2003; Limpert et al., 2004). Although air exhibits much smaller nonlinear refraction coefficient than fused silica, compression of μJ-level pulses encounters onset of nonlinear effects, which degrades the quality of compressed pulses. To date, nearly all the fiber CPA systems with >1 μJ pule energy employ Treacy-type grating pair as the compressor (Bonod and Neauport, 2016). In a fiber CPA system, special attention should be paid to the precise compensation of TOD in order to ensure high-quality pulse compression. Fortunately, several groups demonstrated that intentionally accumulating a certain amount of nonlinear phase shift can mitigate the effect of TOD and improve the compressed-pulse quality (Kalaycioglu et al., 2010; Kuznetsova and Wise, 2007; Shah et al., 2005; Zhou et al., 2005). Thanks to the rapid development of double-clad Yb-doped LMA fibers, femtosecond pulses centered at ~1.03 μm with >100 μJ pulse energy can be routinely obtained in an Yb-fiber CPA system. The blue triangles in Figure 4 show the representative Yb-fiber CPA systems (Röser et al., 2007; Eidam et al., 2010, 2011; Hao et al., 2009; Kim et al., 2015; Plotner et al., 2017; Roser et al., 2007; Wan et al., 2013; Yu et al., 2016; Zhao et al., 2012; Zhao and Kobayashi, 2016; Ogino et al., 2013). In a practical fiber CPA system, the seeding pulse is stretched at most to a duration of ~2 ns. To avoid the detrimental effect of self-focusing, the peak power of the amplified pulse in a fiber amplifier needs to remain well below the catastrophic threshold power (e.g., 4 MW for linearly polarized pulse amplified in Yb-fiber amplifier). These two factors (i.e., stretched-pulse duration and self-focusing) limit the amplified pulse energy; among reported results, the highest pulse energy obtained from a single Yb-fiber CPA system ("single emitter") is about 2.2 mJ (Eidam et al., 2011).

In addition to pulse energy, average power constitutes another important parameter. Fiber laser systems that can deliver femtosecond pulses featuring both high energy (>1 mJ) and high power (>1 kW) are highly desired by high-field science. Scaling of average power in fiber amplifiers is eventually prevented by the onset of thermal modal instability (Dong, 2013; Jauregui et al., 2012; Smith and Smith, 2011; Ward et al., 2012), which limits the average power to 1 kW for Yb-fiber amplifiers that deliver diffraction-limited beams. To further scaling pulse energy and average power, divided pulse amplification (DPA) (Zhou et al., 2007) and coherent beam combining (CBC) are introduced into fiber CPA systems. A thorough review of this technique can be found in Hanna et al., 2016; Klenke et al., 2018. The red circles in Figure 4 present recent Yb-fiber CPA systems incorporating DPA and CBC (Kienel et al., 2016; Klenke et al., 2013, 2014; Mueller et al., 2020; Muller et al., 2016, 2018; Stark et al., 2019); femtosecond pulses with >100 mJ energy and >10 kW average power are expected in the near future.

One drawback associated with the fiber CPA system lies in the fact that the compressed-pulse duration is typically ≥200 fs limited by gain narrowing and residual dispersion mismatch. Many important applications

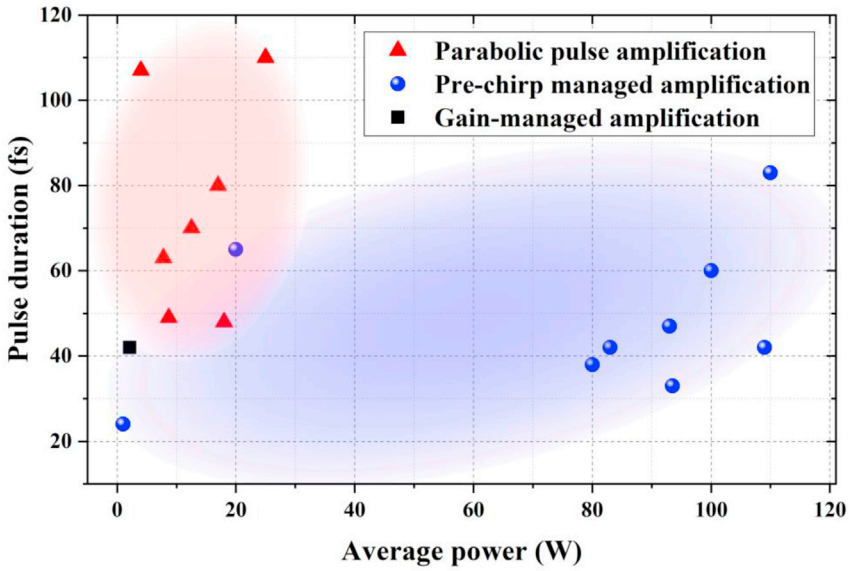


**Figure 5. Pulse Duration as a Function of Average Power for Yb-Fiber Amplifiers Based on Parabolic Pulse Amplification (Red Triangles), PCMA (Blue Circles), and Gain-Managed Amplification (Black Square).**

especially high-field science demand much shorter pulse duration. To meet such duration requirement, subsequent nonlinear pulse compression becomes necessary at the expense of system complexity and throughput efficiency. Depending on the pulse energy offered by a fiber CPA system, the choice of proper nonlinear media can be solid-core LMA fibers (Eidam et al., 2008; Jocher et al., 2012), hollow-core Kagome PCFs (Debord et al., 2014; Guichard et al., 2015), noble gas-filled glass capillaries with sub-mm MFD (Hadrich et al., 2013; Lavenu et al., 2017), and gas-filled multi-pass cell (Lavenu et al., 2019).

### *Nonlinear Amplification*

Some applications, for example, cavity-enhanced high-harmonic generation, demand μJ-level pulses with <100 fs pulse duration and tens-of-MHz repetition rate (Cingöz et al., 2012; Gohle et al., 2005; Jones et al., 2005). Such a parameter combination can be achieved via nonlinear amplification; that is, the amplified pulse is transform limited or slightly stretched in duration (normally <1 ps) and accumulates enough nonlinear phase shift during amplification resulting in significantly broadened spectrum to overcome the gain narrowing effect. At the output, the amplified and spectrally broadened pulse is compressed to a duration much shorter than the seeding pulse.

Indeed, before the invention of CPA (Strickland and Mourou, 1985), pulse amplification without a stretcher was commonly used. Nonlinear amplification was proposed in 1974, which theoretically demonstrated that, after being amplified in a 2-m-long Nd:glass chain, the initial 1-ns pulse can be compressed down to 125 ps due to SPM-caused spectral broadening in the gain medium (Fisher and Bischel, 1974). However, in reality, the short length (<1 cm) of a solid-state gain medium and the absence of waveguide effect in a bulk material give rise to minimal nonlinear phase shift and spectral broadening. This direct pulse amplification technique unsurprisingly died out in the competition with CPA for solid-state amplifiers. After almost 30 years, this technique revived in fiber amplifiers, in which the interplay of positive GVD, SPM, and gain leads to parabolic similariton with a linear chirp, as we show in section "Parabolic Similariton Asymptotically Developed in Fiber Amplifier." Such amplified and linearly chirped pulse can be readily compressed by a Treacy-type grating pair. Known as parabolic pulse amplification, which was first demonstrated in 1996 (Tamura and Nakazawa, 1996), this technique was not fully explored until the theoretical discovery and experimental verification of the self-similar solution of an amplified NLSE in 2000 (Fermann et al., 2000). Since then, parabolic pulse amplification has been demonstrated in Yb-doped fiber amplifiers (Deng et al., 2009; Limpert et al., 2002; Malinowski et al., 2004; Papadopoulos et al., 2007; Zaouter et al., 2007, 2008) as well as Er-doped fiber amplifiers constructed from dispersion shifted fiber (Nicholson et al., 2004; Ozeki et al., 2004, 2005). The red triangles in Figure 5 show the representative results from Yb-fiber

parabolic-pulse-amplification system. This amplification scheme has produced sub-50-fs pulses with ~20 W average power and ~300 nJ pulse energy (Deng et al., 2009).

Further energy scaling of parabolic pulse amplification is prevented by finite gain bandwidth for a short gain fiber and by the onset of stimulated Raman scattering for a long gain fiber (Chang et al., 2004; Soh et al., 2006a, 2006b). The typical active-fiber length in a parabolic pulse amplifier is several meters such that the initial pulse asymptotically evolves into the self-similar regime. On the other hand, construction of the last-stage power amplifier tends to employ short-length (<1 m) active fiber in order to reduce nonlinearity and thus increase amplified pulse energy. Unable to evolve into a parabolic similariton, the amplified pulse in high-gain short-length fiber amplifiers is spectrally broadened beyond the gain bandwidth and develops nonlinear chirp. As a result, the compressed-pulse quality is compromised. In 2012, we proposed and demonstrated that fine pre-chirping the seeding pulse chirp prior to nonlinear amplification generated high-quality compressed pulse (Chen et al., 2012a). We refer to this new application technique as pre-chirp managed amplification (PCMA) (Chen et al., 2012a). Using an Yb-doped rod-type LPF as the power amplifier, PCMA allows generation of μJ-level ultrashort pulses with ~40 fs pulse duration and >100 W average power. The blue circles in Figure 5 summarize typical Yb-fiber PCMA systems (Huang et al., 2016; Liu et al., 2015a; Luo et al., 2016, 2018; Song et al., 2017; Wang et al., 2016; Zhao et al., 2014; Huang et al., 2019; Wu et al., 2013). Thanks to pre-chirp management, which adds one more degree of freedom, PCMA can generate amplified pulses with broader spectrum compared with parabolic pulse amplification. As a result, PCMA has the potential to deliver μJ-level pulses with the duration as short as few optical cycles. Recently a new nonlinear amplification technique was proposed, in which the spectral broadening was managed by longitudinally evolving gain shaping (Sidorenko et al., 2019); as a proof of principle, 42-fs compressed pulses were obtained (black square in Figure 5).

## Wavelength Tuning

It is well known that, among solid-state ultrafast lasers, mode-locked Ti:sapphire laser may be the most successful one largely because the associated huge gain bandwidth permits broadly tuning (>300 nm) the center wavelength of the emitted pulses. Ultrashort pulses with the center wavelength tunable are desired in many microscopy and spectroscopy applications (Lefort, 2017; Taylor, 2016; Tu and Boppart, 2013). Unfortunately, limited by the available gain bandwidth, ultrafast fiber lasers exhibit much narrower tuning range (Ma et al., 2019; Nyushkov et al., 2019). Largely driven by biomedical imaging applications (e.g., multiphoton microscopy), the past decade has witnessed growing research endeavors in developing nonlinear fiber-optic methods to derive wavelength-tunable ultrashort pulses from a source fiber laser. These methods include fiber optical parametric oscillators (OPOs) (Brinkmann et al., 2019; Gottschall et al., 2015; Yang et al., 2018; Zhou et al., 2009), dispersive wave (DW) generation (or so-called Cherenkov radiation) (Chan et al., 2014; Chen et al., 2013; Li et al., 2016; Tauser et al., 2004; Tu et al., 2013; Wang et al., 2015), soliton self-frequency shift (SSFS) (Cadroas et al., 2017; Deng et al., 2015; Fang et al., 2013; Li et al., 2018a; Lim et al., 2014; Rishøj et al., 2019; Takayanagi et al., 2006; van Howe et al., 2007; Yao et al., 2015; Lim et al., 2004), and SPM-enabled spectral selection (SESS) (Chung et al., 2017, 2018; Liu et al., 2016a, 2017a; Niu et al., 2018; Yu et al., 2019). They can significantly expand the wavelength coverage of ultrafast fiber lasers. Table 3 summarizes the representative results including wavelength tuning range, maximum pulse energy, pulse duration, repetition rate, and excitation wavelength. To have a better comparison, Figure 6 plots the maximum pulse energy obtained by nonlinear fiber-optical wavelength conversion as a function of wavelength tuning range. In this figure, we only show the results corresponding to >1 nJ pulse energy.

Fiber OPOs employ four-wave mixing inside an optical fiber and exhibit certain wavelength tunability (up to ~180 nm). Fiber dispersion gives rise to narrow phase-matching bandwidth, which limits the generated pulse duration and often results in sub-picosecond or picosecond pulses. For example, a fiber OPO pumped by a μJ-level Yb-fiber laser system produces 27-nJ, 560-fs pulses post compression (Gottschall et al., 2015).

Dispersive wave generation as described earlier can generate femtosecond pulses with a duration well below 100 fs. In most cases, the optical fiber exhibits positive TOD and the dispersive-wave pulse has a center wavelength shorter than the excitation pulse. For example, we demonstrated that dispersive-wave pulses centered at 850 nm with 200-nm bandwidth were derived from a 3-GHz Yb-fiber laser system and double-chirped mirrors dechirped these pulses down to 14 fs in duration (Chen et al., 2013). However, as Equation 5 shows, the center wavelength of the generated dispersive wave is mainly determined by the fiber dispersion. Both theoretical and experimental results showed that varying the input pulse peak power can at best tune the center wavelength of the dispersive wave by about 100 nm (Chang et al.,

| | Tuning Range (μm) | Max. Energy (nJ) | Pulse Duration (fs) | Repetition Rate (MHz) | Excitation Wavelength (μm) |
|---|---|---|---|---|---|
| Fiber OPO | 1.2–1.3 | 27 | >560 | 0.785 | 1.04 |
| | 0.78–0.98 | 10 | 7,000 | 40.5 | 1.04 |
| | 1.41–1.54 | 0.03 | 10,200 | 156.2 | 1.54–1.56 |
| | 1.57–1.69 | 125 | 350 | 0.8–20 | 1.06 |
| Dispersive wave generation | 0.96–1.02 | 0.23 | <25 | 67 | 1.55 |
| | 1.13–1.3 | 0.13 | 14 | 3,000 | 1.03 |
| | 0.75–0.95 | 2.3 | 25 | 50 | 1.55 |
| | 0.37–0.85 | >4 | >404 | 54.77 | 1.03 |
| | 0.6–0.8 | 1.05 | 125 | 52.4 | 1.55 |
| SSFS at fundamental mode | 1.2–1.3 | 0.5 | <100 | 60 | 1 |
| | 1.03–1.33 | 0.24 | 100–150 | 41.3 | 1.05 |
| | 1.05–1.69 | 73 | 100 | 0.66 | 1.55 |
| | 1.58–2.52 | 6.4 | 82 | 50 | 1.04 |
| | 1.16–1.26 | 0.3 | 136 | 3,000 | 1.03 |
| | 1.15–1.35 | 3 | NA | 39.6 | 1.03 |
| | 1.2–1.28 | 9 | 75 | 50 | 1.56 |
| | 1.6–1.7 | 13.1 | <100 | 38.2 | 1.55 |
| SSFS in HOM fibers | 1.58–2.07 | 0.8 | 49 | 80 | 1.06 |
| | 1.05–1.6 | 80 | 74 | NA | 1.04 |
| SESS | 1.04–1.6 | 3.3 | 70–120 | 55 | 1.03 |
| | 0.82–1.21 | 22 | 50–90 | 55 | 1.03 |
| | 1.03–1.21 | 10 | 50 | 31 | 1.55 |
| | 1.3–1.7 | 130 | 100 | 31 | 1.55 |
| | 1.3–1.7 | 10.1 | 80–117 | 37 | 1.03 |
| | 0.92–1.03 | 33 | 100 | 1 | 1.03 |

**Table 3. Nonlinear Fiber-Optic Methods for Wavelength Conversion**

2010; Wang et al., 2015). Increasing the wavelength tuning range can be achieved using several fibers with different zero-dispersion wavelength (Tu et al., 2013). Reference Liu et al. (2015b) presents a thorough review of dispersive wave generation excited by ultrafast fiber lasers.

SSFS can generate femtosecond Raman soliton pulses with the center wavelength continuously red-shifted by varying the input pulse energy. The pulse energy of a Raman soliton needs to satisfy the well-known soliton area theorem (Equation 4), which shows that the pulse energy is proportional to $A_{eff}$, the fiber MFA. SFSS requires negative GVD to form Raman soliton, and therefore ultrafast Yb-fiber lasers cannot be used to excite SSFS in conventional single-mode fibers that exhibit positive GVD for wavelength <1.03 μm. Instead, PCFs with a small MFD (<3 μm) can offer negative GVD for the excitation pulses at ~1.03 μm. The associated strong nonlinearity in these PCFs limits the Raman soliton pulse energy to ~0.1 nJ. The conflict between negative GVD and large MFA in a single-mode fiber is resolved by higher-order-mode (HOM) fibers because they can exhibit negative GVD as well as have a large MFA. SSFS in HOM fibers allows generation of energetic Raman solitons with up to 80 nJ pulse energy pumped by Yb-fiber lasers (Rishøj et al., 2019; van Howe et al., 2007). Ultrafast Er-fiber lasers can be used to excite SSFS at the fundamental mode in LMA fibers. For example, using 1550-nm femtosecond

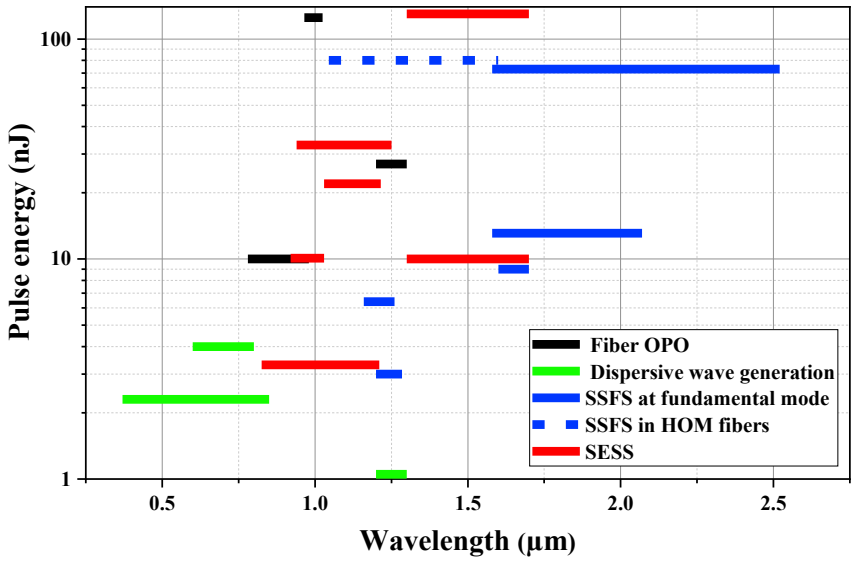


**Figure 6. Maximum Pulse Energy versus Wavelength Tuning Range for Different Nonlinear Fiber-optic Methods**

pulses from an Er-fiber laser system as the excitation pulses, ~100-fs pulses tunable in 1,580–2,520 nm with up to 70 nJ pulse energy were obtained (Yu et al., 2019).

SESS constitutes a new fiber-optic wavelength conversion method featuring large wavelength tuning range (>400 nm) and superior energy scalability (Liu et al., 2016a, 2017a). SESS employs SPM-dominated nonlinearity in a short fiber to dramatically broaden an input narrowband optical spectrum to a broadband spectrum comprising well-isolated spectral lobes. A considerable portion of power is contained by the leftmost and the rightmost spectral lobes, which are selected by proper optical filters to produce nearly transform-limited femtosecond pulses (without external compression) with the center wavelength widely tunable. Excited in a PCF by an Yb-fiber ultrafast laser, SESS generated ~100-fs pulses tunable from 825 to 1,210 nm with >1 nJ pulse energy (Liu et al., 2016a). The SESS pulse energy can be scaled up by using shorter fiber with a larger MFA. Using 8-cm LMA fiber with 7.5-μm MFD, we demonstrated a SESS source that produced ~100-fs pulses tunable from 940 to 1,250 nm with up to 33 nJ pulse energy (Yu et al., 2019). To cover the two transmission windows (i.e., 1.3 and 1.7 μm) for biomedical microscopy imaging, we employed a high-power ultrafast Er-fiber MOPA system to excite SESS and achieved ~100-fs pulses tunable in 1.3–1.7 μm (Chung et al., 2017, 2018). We also showed that the SESS pulse energy can be scaled up to 130 nJ, leading to wavelength tunable pulses with >1 MW peak power (Chung et al., 2017). Using such a SESS source to drive multimodal multiphoton microscopy imaging, we have performed optical virtual biopsy in human skin (Chung et al., 2019a, 2019b).

## CONCLUSION AND OUTLOOK

Ultrafast fiber lasers undeniably constitute a powerful toolbox, which provides solution to various scientific and industrial problems. The versatility and capability of such toolbox relies heavily on the parameter space that ultrafast fiber lasers can access. In this paper, we reviewed recent progress in this fertile research field with a focus on improving laser parameters such as repetition rate, pulse energy, average power, pulse duration, and wavelength tuning range. A subset of these parameters defines the performance of an ultrafast fiber laser aiming for a specific application.

We restricted our discussion to ultrafast Yb-fiber and Er-fiber laser systems that operate at the near-infrared wavelength range. As Figure 1 indicates, ultrafast Tm-fiber and Ho-fiber lasers operating at ~2 μm have received increased research interest and progressed at a rapid pace. To generate femtosecond pulses at even longer wavelength directly from a laser, a passively mode-locked $Er^{3+}$: fluoride glass fiber oscillator was demonstrated, which delivered 207-fs pulses at 2.8 μm (Duval et al., 2015). In addition to the emergence of new active fibers that bring forth ultrafast fiber lasers emitting at new wavelength (Zhu et al.,

2017), remarkable advances appear in the development of passive fibers that are fabricated from new glass materials or designed with novel structures. We strongly believe that the continuous progress in both active and passive fibers will promote new techniques to further expand the toolbox of ultrafast fiber lasers, which will in turn solve the challenges faced by existing and emerging applications.

## METHODS

All methods can be found in the accompanying Transparent Methods supplemental file.

## ACKNOWLEDGMENTS

We acknowledge support by the Guangdong Key-area R&D Program (No.2018B090904003), National Key R&D Program of China (No.2018YFB1107200), and the National Natural Science Foundation of China (No.11774234, No.91850209).

## AUTHOR CONTRIBUTIONS

G. C. and Z. W. conceived the review topic and outlined the manuscript. G. C. wrote the manuscript and Z. W. edited the manuscript.

## REFERENCES

Agrawal, G. (2006). Nonlinear Fiber Optics (Academic Press).

Akhmediev, N., and Karlsson, M. (1995). Cherenkov radiation emitted by solitons in optical fibers. Phys. Rev. A *51*, 2602–2607.

Akosman, A.E., and Sander, M.Y. (2017). Dual comb generation from a mode-locked fiber laser with orthogonally polarized interlaced pulses. Opt. Express *25*, 18592–18602.

Anderson, D., Desaix, M., Lisak, M., and Quiroga–Teixeiro, M.L. (1992). Wave breaking in nonlinear-optical fibers. J. Opt. Soc. Am. B *9*, 1358–1361.

Austin, D.R., de Sterke, C.M., Eggleton, B.J., and Brown, T.G. (2006). Dispersive wave blue-shift in supercontinuum generation. Opt. Express *14*, 11997–12007.

Bao, Q., Zhang, H., Wang, Y., Ni, Z., Yan, Y., Shen, Z.X., Loh, K.P., and Tang, D.Y. (2009). Atomic-Layer graphene as a saturable absorber for ultrafast pulsed lasers. Adv. Funct. Mater. *19*, 3077–3083.

Birks, T.A., Mogilevtsev, D., Knight, J.C., and Russell, P.S.J. (1999). Dispersion compensation using single-material fibers. IEEE Photon. Technol. Lett. *11*, 674–676.

Bonod, N., and Neauport, J. (2016). Diffraction gratings: from principles to applications in high-intensity lasers. Adv. Opt. Photon. *8*, 156–199.

Boscolo, S., Turitsyn, S.K., Novokshenov, V.Y., and Nijhof, J.H.B. (2002). Self-similar parabolic optical solitary waves. Theor. Math. Phys. *133*, 1647–1656.

Brida, D., Krauss, G., Sell, A., and Leitenstorfer, A. (2014). Ultrabroadband Er: fiber lasers. Laser Photon. Rev. *8*, 409–428.

Brinkmann, M., Fast, A., Hellwig, T., Pence, I., Evans, C.L., and Fallnich, C. (2019). Portable all-fiber dual-output widely tunable light source for coherent Raman imaging. Biomed. Opt. Express *10*, 4437–4449.

Byun, H., Sander, M.Y., Motamedi, A., Shen, H., Petrich, G.S., Kolodziejski, L.A., Ippen, E.P., and Kartner, F.X. (2010). Compact, stable 1 GHz femtosecond Er-doped fiber lasers. Appl. Opt. *49*, 5577–5582.

Cadroas, P., Abdeladim, L., Kotov, L., Likhachev, M., Lipatov, D., Gaponov, D., Hideur, A., Tang, M., Livet, J., Supatto, W., et al. (2017). All-fiber femtosecond laser providing 9 nJ, 50 MHz pulses at 1650 nm for three-photon microscopy. J. Opt. *19*, 065506.

Chan, M.C., Lien, C.H., Lu, J.Y., and Lyu, B.H. (2014). High power NIR fiber-optic femtosecond Cherenkov radiation and its application on nonlinear light microscopy. Opt. Express *22*, 9498–9507.

Chang, G., Chen, L.-J., and Kärtner, F.X. (2010). Highly efficient Cherenkov radiation in photonic crystal fibers for broadband visible wavelength generation. Opt. Lett. *35*, 2361–2363.

Chang, G., Chen, L.-J., and Kärtner, F.X. (2011). Fiber-optic Cherenkov radiation in the few-cycle regime. Opt. Express *19*, 6635–6647.

Chang, G., Galvanauskas, A., Winful, H.G., and Norris, T.B. (2004). Dependence of parabolic pulse amplification on stimulated Raman scattering and gain bandwidth. Opt. Lett. *29*, 2647–2649.

Chang, G., Rever, M., Smirnov, V., Glebov, L., and Galvanauskas, A. (2009). Femtosecond Yb-fiber chirped-pulse-amplification system based on chirped-volume Bragg gratings. Opt. Lett. *34*, 2952–2954.

Chang, G., Winful, H.G., Galvanauskas, A., and Norris, T.B. (2005). Self-similar parabolic beam generation and propagation. Phys. Rev. E *72*, 016609.

Chang, G., Winful, H.G., Galvanauskas, A., and Norris, T.B. (2006). Incoherent self-similarities of the coupled amplified nonlinear Schrödinger equations. Phys. Rev. E *73*, 016616.

Chen, H.-W., Lim, J., Huang, S.-W., Schimpf, D.N., Kärtner, F.X., and Chang, G. (2012a). Optimization of femtosecond Yb-doped fiber amplifiers for high-quality pulse compression. Opt. Express *20*, 28672–28682.

Chen, H.W., Chang, G., Xu, S., Yang, Z., and Kartner, F.X. (2012b). 3 GHz, fundamentally mode-locked, femtosecond Yb-fiber laser. Opt. Lett. *37*, 3522–3524.

Chen, H.W., Haider, Z., Lim, J., Xu, S., Yang, Z., Kartner, F.X., and Chang, G. (2013). 3 GHz, Yb-fiber laser-based, few-cycle ultrafast source at the Ti:sapphire laser wavelength. Opt. Lett. *38*, 4927–4930.

Chen, J., Sickler, J.W., Ippen, E.P., and Kartner, F.X. (2007). High repetition rate, low jitter, low intensity noise, fundamentally mode-locked 167 fs soliton Er-fiber laser. Opt. Lett. *32*, 1566–1568.

Chen, J., Zhao, X., Yao, Z., Li, T., Li, Q., Xie, S., Liu, J., and Zheng, Z. (2019). Dual-comb spectroscopy of methane based on a free-running Erbium-doped fiber laser. Opt. Express *27*, 11406–11412.

Cheng, H., Wang, W., Zhou, Y., Qiao, T., Lin, W., Guo, Y., Xu, S., and Yang, Z. (2018). High-repetition-rate ultrafast fiber lasers. Opt. Express *26*, 16411–16421.

Cheng, H., Wang, W., Zhou, Y., Qiao, T., Lin, W., Xu, S., and Yang, Z. (2017). 5 GHz fundamental repetition rate, wavelength tunable, all-fiber passively mode-locked Yb-fiber laser. Opt. Express *25*, 27646–27651.

Chong, A., Renninger, W.H., and Wise, F.W. (2008). Properties of normal-dispersion femtosecond fiber lasers. J. Opt. Soc. Am. B *25*, 140–148.

Chong, A., Wright, L.G., and Wise, F.W. (2015). Ultrafast fiber lasers based on self-similar pulse evolution: a review of current progress. Rep. Prog. Phys. *78*, 113901.

Chung, H., Liu, W., Cao, Q., Greinert, R., Kärtner, F.X., and Chang, G. (2019a). Tunable, ultrafast fiber-laser between 1.15 and 1.35 μm for harmonic generation microscopy in human skin. IEEE J. Sel. Top. Quantum Electron. *25*, 1–8.

Chung, H.-Y., Greinert, R., Kärtner, F.X., and Chang, G. (2019b). Multimodal imaging platform for optical virtual skin biopsy enabled by a fiber-based two-color ultrafast laser source. Biomed. Opt. Express *10*, 514–525.

Chung, H.-Y., Liu, W., Cao, Q., Song, L., Kärtner, F.X., and Chang, G. (2018). Megawatt peak power tunable femtosecond source based on self-phase modulation enabled spectral selection. Opt. Express *26*, 3684–3695.

Chung, H.Y., Liu, W., Cao, Q., Kartner, F.X., and Chang, G. (2017). Er-fiber laser enabled, energy scalable femtosecond source tunable from 1.3 to 1.7 microm. Opt. Express *25*, 15760–15771.

Cingöz, A., Yost, D.C., Allison, T.K., Ruehl, A., Fermann, M.E., Hartl, I., and Ye, J. (2012). Direct frequency comb spectroscopy in the extreme ultraviolet. Nature *482*, 68–71.

Coddington, I., Newbury, N., and Swann, W. (2016). Dual-comb spectroscopy. Optica *3*, 414–426.

Cristiani, I., Tediosi, R., Tartara, L., and Degiorgio, V. (2004). Dispersive wave generation by solitons in microstructured optical fibers. Opt. Express *12*, 124–135.

Cui, Y., and Liu, X. (2013). Graphene and nanotube mode-locked fiber laser emitting dissipative and conventional solitons. Opt. Express *21*, 18969–18974.

de Matos, C.J.S., Taylor, J.R., Hansen, T.P., Hansen, K.P., and Broeng, J. (2003). All-fiber chirped pulse amplification using highly-dispersive air-core photonic bandgap fiber. Opt. Express *11*, 2832–2837.

Debord, B., Alharbi, M., Vincetti, L., Husakou, A., Fourcade-Dutin, C., Hoenninger, C., Mottay, E., Gérôme, F., and Benabid, F. (2014). Multi-meter fiber-delivery and pulse self-compression of milli-Joule femtosecond laser and fiber-aided laser-micromachining. Opt. Express *22*, 10735–10746.

Deng, D., Cheng, T., Xue, X., Tong, H.T., Suzuki, T., and Ohishi, Y. (2015). Widely tunable soliton self-frequency shift and dispersive wave generation in a highly nonlinear fiber. Optical Components and Materials XII*9359* (SPIE).

Deng, Y., Chien, C.-Y., Fidric, B.G., and Kafka, J.D. (2009). Generation of sub-50 fs pulses from a high-power Yb-doped fiber amplifier. Opt. Lett. *34*, 3469–3471.

Deng, Z., Liu, Y., Ouyang, C., Zhang, W., Wang, C., and Li, W. (2019). Mutually coherent dual-comb source generated from a free-running linear fiber laser. Results Phys. *14*, 102364.

Dong, L. (2013). Stimulated thermal Rayleigh scattering in optical fibers. Opt. Express *21*, 2642–2656.

Dong, L., Wu, T., McKay, H.A., Fu, L., Li, J., and Winful, H.G. (2009). All-glass large-core leakage channel fibers. IEEE J. Sel. Top. Quantum Electron. *15*, 47–53.

Doran, N.J., and Wood, D. (1988). Nonlinear-optical loop mirror. Opt. Lett. *13*, 56–58.

Du, W., Xia, H., Li, H., Liu, C., Wang, P., and Liu, Y. (2017). High-repetition-rate all-fiber femtosecond laser with an optical integrated component. Appl. Opt. *56*, 2504–2509.

Dudley, J.M., Finot, C., Richardson, D.J., and Millot, G. (2007). Self-similarity in ultrafast nonlinear optics. Nat. Phys. *3*, 597–603.

Duval, S., Bernier, M., Fortin, V., Genest, J., Piché, M., and Vallée, R. (2015). Femtosecond fiber lasers reach the mid-infrared. Optica *2*, 623–626.

Dzhibladze, M.I., Ésiashvili, Z.G., Teplitskiĭ, E.S., Isaev, S.K., and Sagaradze, V.R. (1983). Mode locking in a fiber laser. Soviet Journal of Quantum Electronics *13*, 245–247.

Eidam, T., Hanf, S., Seise, E., Andersen, T.V., Gabler, T., Wirth, C., Schreiber, T., Limpert, J., and Tuennermann, A. (2010). Femtosecond fiber CPA system emitting 830 W average output power. Opt. Lett. *35*, 94–96.

Eidam, T., Röser, F., Schmidt, O., Limpert, J., and Tünnermann, A. (2008). 57 W, 27 fs pulses from a fiber laser system using nonlinear compression. Appl. Phys. B *92*, 9.

Eidam, T., Rothhardt, J., Stutzki, F., Jansen, F., Haedrich, S., Carstens, H., Jauregui, C., Limpert, J., and Tuennermann, A. (2011). Fiber chirped-pulse amplification system emitting 3.8 GW peak power. Opt. Express *19*, 255–260.

Fang, X.-H., Hu, M.-L., Liu, B.-W., Chai, L., Wang, C.-Y., Wei, H.-F., Tong, W.-J., Luo, J., Sun, C.-K., Voronin, A.A., et al. (2013). An all-photonic-crystal-fiber wavelength-tunable source of high-energy sub-100fs pulses. Opt. Commun. *289*, 123–126.

Fermann, M.E., Andrejco, M.J., Silberberg, Y., and Stock, M.L. (1993). Passive mode locking by using nonlinear polarization evolution in a polarization-maintaining erbium-doped fiber. Opt. Lett. *18*, 894–896.

Fermann, M.E., Haberl, F., Hofer, M., and Hochreiter, H. (1990a). Nonlinear amplifying loop mirror. Opt. Lett. *15*, 752–754.

Fermann, M.E., and Hartl, I. (2009). Ultrafast fiber laser technology. IEEE J. Sel. Top. Quantum Electron. *15*, 191–206.

Fermann, M.E., and Hartl, I. (2013). Ultrafast fibre lasers. Nat. Photon. *7*, 868–874.

Fermann, M.E., Hofer, M., Haberl, F., and Craig-Ryan, S.P. (1990b). Femtosecond fibre laser. Electronics Letters *26*, 1737–1738.

Fermann, M.E., Kruglov, V.I., Thomsen, B.C., Dudley, J.M., and Harvey, J.D. (2000). Self-similar propagation and amplification of parabolic pulses in optical fibers. Phys. Rev. Lett. *84*, 6010–6013.

Finot, C., Barviau, B., Millot, G., Guryanov, A., Sysoliatin, A., and Wabnitz, S. (2007). Parabolic pulse generation with active or passive dispersion decreasing optical fibers. Opt. Express *15*, 15824–15835.

Finot, C., Dudley, J.M., Kibler, B., Richardson, D.J., and Millot, G. (2009). Optical parabolic pulse generation and applications. IEEE J. Quantum Electron. *45*, 1482–1489.

Finot, C., Millot, G., Billet, C., and Dudley, J.M. (2003). Experimental generation of parabolic pulses via Raman amplification in optical fiber. Opt. Express *11*, 1547–1552.

Fisher, R.A., and Bischel, W.K. (1974). Pulse compression for more efficient operation of solid-state laser amplifier chains. Appl. Phys. Lett. *24*, 468–470.

Galvanauskas, A. (2001). Mode-scalable fiber-based chirped pulse amplification systems. IEEE J. Sel. Top. Quantum Electron. *7*, 504–517.

Gohle, C., Udem, T., Herrmann, M., Rauschenberger, J., Holzwarth, R., Schuessler, H.A., Krausz, F., and Hänsch, T.W. (2005). A frequency comb in the extreme ultraviolet. Nature *436*, 234–237.

Gordon, J.P. (1986). Theory of the soliton self-frequency shift. Opt. Lett. *11*, 662–664.

Gottschall, T., Meyer, T., Schmitt, M., Popp, J., Limpert, J., and Tünnermann, A. (2015). Four-wave-mixing-based optical parametric oscillator delivering energetic, tunable, chirped femtosecond pulses for non-linear biomedical applications. Opt. Express *23*, 23968–23977.

Guichard, F., Giree, A., Zaouter, Y., Hanna, M., Machinet, G., Debord, B., Gérôme, F., Dupriez, P., Druon, F., Hönninger, C., et al. (2015). Nonlinear compression of high energy fiber amplifier pulses in air-filled hypocycloid-core Kagome fiber. Opt. Express *23*, 7416–7423.

Guo, J., Ding, Y., Xiao, X., Kong, L., and Yang, C. (2018). Multiplexed static FBG strain sensors by dual-comb spectroscopy with a free running fiber laser. Opt. Express *26*, 16147–16154.

Guo, J., Zhao, K., Zhou, B., Ning, W., Jiang, K., Yang, C., Kong, L., and Dai, Q. (2019). Wearable and skin-mountable fiber-optic strain sensors interrogated by a free-running, dual-comb fiber laser. Adv. Opt. Mater. *7*, 1900086.

Hadrich, S., Klenke, A., Hoffmann, A., Eidam, T., Gottschall, T., Rothhardt, J., Limpert, J., and Tunnermann, A. (2013). Nonlinear compression to sub-30-fs, 0.5 mJ pulses at 135 W of average power. Opt. Lett. *38*, 3866–3869.

Hanna, M., Guichard, F., Zaouter, Y., Papadopoulos, D.N., Druon, F., and Georges, P. (2016). Coherent combination of ultrafast fiber amplifiers. J. Phys. B At. Mol. Opt. Phys. *49*, 062004.

Hänsel, W., Hoogland, H., Giunta, M., Schmid, S., Steinmetz, T., Doubek, R., Mayer, P., Dobner, S., Cleff, C., Fischer, M., et al. (2017). All polarization-maintaining fiber laser architecture for robust femtosecond pulse generation. Appl. Phys. B *123*, 1–6.

Hao, Q., Li, W., and Zeng, H. (2009). High-power Yb-doped fiber amplification system synchronized with a few-cycle Ti:sapphire laser. Opt. Express *17*, 5815–5821.

Hill, K.O., Bilodeau, F., Malo, B., Kitagawa, T., Thériault, S., Johnson, D.C., Albert, J., and Takiguchi, K. (1994). Chirped in-fiber Bragg gratings for compensation of optical-fiber dispersion. Opt. Lett. *19*, 1314–1316.

Hirooka, T., and Nakazawa, M. (2004). Parabolic pulse generation by use of a dispersion-decreasing fiber with normal group-velocity dispersion. Opt. Lett. *29*, 498–500.

Hong, S., Lédée, F., Park, J., Song, S., Lee, H., Lee, Y.S., Kim, B., Yeom, D.-I., Deleporte, E., and Oh, K. (2018). Mode-locking of all-fiber lasers operating at both anomalous and normal dispersion regimes in the C- and L-bands using thin film of 2D perovskite crystallites. Laser Photon. Rev. *12*, 1800118.

Hu, G., Mizuguchi, T., Oe, R., Nitta, K., Zhao, X., Minamikawa, T., Li, T., Zheng, Z., and Yasui, T. (2018). Dual terahertz comb spectroscopy with a single free-running fibre laser. Sci. Rep. *8*, 11155.

Hu, G., Mizuguchi, T., Zhao, X., Minamikawa, T., Mizuno, T., Yang, Y., Li, C., Bai, M., Zheng, Z., and Yasui, T. (2017). Measurement of absolute frequency of continuous-wave terahertz radiation in real time using a free-running, dual-wavelength mode-locked, erbium-doped fibre laser. Sci. Rep. *7*, 42082.

Huang, H., Zhang, Y., Teng, H., Fang, S., Wang, J., Zhu, J., Kaertner, F., Chang, G., Wei, Z., and IEEE. (2019). Pre-chirp managed amplification of circularly polarized pulses using chirped mirrors for pulse compression. In 2019 Conference on Lasers and Electro-Optics.

Huang, L., Zhou, Y., Dai, Y., Yin, F., Dai, J., and Xu, K. (2017). 1-GHz, compact mode locked femtosecond all-polarization maintaining erbium-doped fiber oscillator. Paper presented at: 2017 International Topical Meeting on Microwave Photonics (MWP).

Huang, L.-l., Hu, M.-l., Fang, X.-h., Liu, B.-w., Chai, L., and Wang, C.-y. (2016). Generation of 110-W sub-100-fs pulses at 100 MHz by nonlinear amplification based on multicore photonic crystal fiber. IEEE Photon. J. *8*, 1–7.

Hundertmark, H., Kracht, D., Engelbrecht, M., Wandt, D., and Fallnich, C. (2004). Stable sub-85 fs passively mode-locked Erbium-fiber oscillator with tunable repetition rate. Opt. Express *12*, 3178–3183.

Husakou, A.V., and Herrmann, J. (2001). Supercontinuum generation of higher-order solitons by fission in photonic crystal fibers. Phys. Rev. Lett. *87*, 203901.

Ideguchi, T., Poisson, A., Guelachvili, G., Picqué, N., and Hänsch, T.W. (2014). Adaptive real-time dual-comb spectroscopy. Nat. Commun. *5*, 3375.

Ilday, F., Chen, J., and Kartner, F. (2005). Generation of sub-100-fs pulses at up to 200 MHz repetition rate from a passively mode-locked Yb-doped fiber laser. Opt. Express *13*, 2716–2721.

Ilday, F.Ö., Buckley, J.R., Clark, W.G., and Wise, F.W. (2004). Self-similar evolution of parabolic pulses in a laser. Phys. Rev. Lett. *92*, 213902.

Jackson, S.D. (2012). Towards high-power mid-infrared emission from a fibre laser. Nat. Photon. *6*, 423–431.

Jauregui, C., Eidam, T., Otto, H.-J., Stutzki, F., Jansen, F., Limpert, J., and Tünnermann, A. (2012). Physical origin of mode instabilities in high-power fiber laser systems. Opt. Express *20*, 12912–12925.

Jauregui, C., Limpert, J., and Tünnermann, A. (2013). High-power fibre lasers. Nat. Photon. *7*, 861–867.

Jiang, T., Cui, Y., Lu, P., Li, C., Wang, A., and Zhang, Z. (2016). All PM fiber laser mode locked with a compact phase biased amplifier loop mirror. IEEE Photon. Technol. Lett. *28*, 1786–1789.

Jin, X., Zhang, M., Hu, G., Wu, Q., Zheng, Z., and Hasan, T. (2020). Broad bandwidth dual-wavelength fiber laser simultaneously delivering stretched pulse and dissipative soliton. Opt. Express *28*, 6937–6944.

Jocher, C., Eidam, T., Hadrich, S., Limpert, J., and Tunnermann, A. (2012). Sub 25 fs pulses from solid-core nonlinear compression stage at 250 W of average power. Opt. Lett. *37*, 4407–4409.

Jones, R.J., Moll, K.D., Thorpe, M.J., and Ye, J. (2005). Phase-coherent frequency combs in the vacuum ultraviolet via high-harmonic generation inside a femtosecond enhancement cavity. Phys. Rev. Lett. *94*, 193201.

Kalaycioglu, H., Oktem, B., Şenel, Ç., Paltani, P.P., and Ilday, F.Ö. (2010). Microjoule-energy, 1 MHz repetition rate pulses from all-fiber-integrated nonlinear chirped-pulse amplifier. Opt. Lett. *35*, 959–961.

Karpman, V.I. (1993). Radiation by solitons due to higher-order dispersion. Phys. Rev. E *47*, 2073–2082.

Kayes, M.I., Abdukerim, N., Rekik, A., and Rochette, M. (2018). Free-running mode-locked laser based dual-comb spectroscopy. Opt. Lett. *43*, 5809–5812.

Keller, U., Knox, W.H., and Roskos, H. (1990). Coupled-cavity resonant passive mode-locked Ti:sapphire laser. Opt. Lett. *15*, 1377–1379.

Keller, U., Weingarten, K.J., Kartner, F.X., Kopf, D., Braun, B., Jung, I.D., Fluck, R., Honninger, C., Matuschek, N., and Au, J.A.d. (1996). Semiconductor saturable absorber mirrors (SESAM's) for femtosecond to nanosecond pulse generation in solid-state lasers. IEEE J. Sel. Top. Quantum Electron. *2*, 435–453.

Kienel, M., Muller, M., Klenke, A., Limpert, J., and Tunnermann, A. (2016). 12 mJ kW-class ultrafast fiber laser system using multidimensional coherent pulse addition. Opt. Lett. *41*, 3343–3346.

Kim, K., Peng, X., Lee, W., Gee, S., Mielke, M., Luo, T., Pan, L., Wang, Q., and Jiang, S. (2015). Monolithic polarization maintaining fiber chirped pulse amplification (CPA) system for high energy femtosecond pulse generation at 1.03 microm. Opt. Express *23*, 4766–4770.

Klenke, A., Breitkopf, S., Kienel, M., Gottschall, T., Eidam, T., Hadrich, S., Rothhardt, J., Limpert, J., and Tunnermann, A. (2013). 530 W, 1.3 mJ, four-channel coherently combined femtosecond fiber chirped-pulse amplification system. Opt. Lett. *38*, 2283–2285.

Klenke, A., Hadrich, S., Eidam, T., Rothhardt, J., Kienel, M., Demmler, S., Gottschall, T., Limpert, J., and Tunnermann, A. (2014). 22 GW peak-power fiber chirped-pulse-amplification system. Opt. Lett. *39*, 6875–6878.

Klenke, A., Müller, M., Stark, H., Kienel, M., Jauregui, C., Tünnermann, A., and Limpert, J. (2018). Coherent beam combination of ultrafast fiber lasers. IEEE J. Sel. Top. Quantum Electron. *24*, 1–9.

Kruglov, V.I., Peacock, A.C., Dudley, J.M., and Harvey, J.D. (2000). Self-similar propagation of high-power parabolic pulses in optical fiber amplifiers. Opt. Lett. *25*, 1753–1755.

Kruglov, V.I., Peacock, A.C., Harvey, J.D., and Dudley, J.M. (2002). Self-similar propagation of parabolic pulses in normal-dispersion fiber amplifiers. J. Opt. Soc. Am. B *19*, 461–469.

Kuznetsova, L., and Wise, F.W. (2007). Scaling of femtosecond Yb-doped fiber amplifiers to tens of microjoule pulse energy via nonlinear chirped pulse amplification. Opt. Lett. *32*, 2671–2673.

Lavenu, L., Natile, M., Guichard, F., Délen, X., Hanna, M., Zaouter, Y., and Georges, P. (2019). High-power two-cycle ultrafast source based on hybrid nonlinear compression. Opt. Express *27*, 1958–1967.

Lavenu, L., Natile, M., Guichard, F., Zaouter, Y., Hanna, M., Mottay, E., and Georges, P. (2017). High-energy few-cycle Yb-doped fiber amplifier source based on a single nonlinear compression stage. Opt. Express *25*, 7530–7537.

Lefort, C. (2017). A review of biomedical multiphoton microscopy and its laser sources. J. Phys. D Appl. Phys. *50*, 423001.

Li, B., Wang, M., Charan, K., Li, M.-j., and Xu, C. (2018a). Investigation of the long wavelength limit of soliton self-frequency shift in a silica fiber. Opt. Express *26*, 19637–19647.

Li, C., Ma, Y., Gao, X., Niu, F., Jiang, T., Wang, A., and Zhang, Z. (2015). 1 GHz repetition rate femtosecond Yb:fiber laser for direct generation of carrier-envelope offset frequency. Appl. Opt. *54*, 8350–8353.

Li, C., Wang, G., Jiang, T., Li, P., Wang, A., and Zhang, Z. (2014a). Femtosecond amplifier similariton Yb:fiber laser at a 616 MHz repetition rate. Opt. Lett. *39*, 1831–1833.

Li, C., Wang, G., Jiang, T., Wang, A., and Zhang, Z. (2013). 750 MHz fundamental repetition rate femtosecond Yb:fiber ring laser. Opt. Lett. *38*, 314–316.

Li, K.-C., Huang, L.L.H., Liang, J.-H., and Chan, M.-C. (2016). Simple approach to three-color two-photon microscopy by a fiber-optic wavelength convertor. Biomed. Opt. Express *7*, 4803–4815.

Li, R., Shi, H., Tian, H., Li, Y., Liu, B., Song, Y., and Hu, M. (2018b). All-polarization-maintaining dual-wavelength mode-locked fiber laser based on Sagnac loop filter. Opt. Express *26*, 28302–28311.

Li, X., Zou, W., and Chen, J. (2014b). 41.9 fs hybridly mode-locked Er-doped fiber laser at 212 MHz repetition rate. Opt. Lett. *39*, 1553–1556.

Liao, K.-H., Cheng, M.-Y., Flecher, E., Smirnov, V.I., Glebov, L.B., and Galvanauskas, A. (2007). Large-aperture chirped volume Bragg grating based fiber CPA system. Opt. Express *15*, 4876–4882.

Liao, R., Song, Y., Liu, W., Shi, H., Chai, L., and Hu, M. (2018). Dual-comb spectroscopy with a single free-running thulium-doped fiber laser. Opt. Express *26*, 11046–11054.

Lim, H., Buckley, J., Chong, A., and Wise, F.W. (2004). Fibre-based source of femtosecond

pulses tunable from 1.0 to 1.3 /spl mu/m. Electronics Letters *40*, 1523–1525.

Lim, J., Chen, H.W., Xu, S., Yang, Z., Chang, G., and Kartner, F.X. (2014). 3 GHz, watt-level femtosecond Raman soliton source. Opt. Lett. *39*, 2060–2063.

Limpert, J., Deguil-Robin, N., Manek-Hönninger, I., Salin, F., Röser, F., Liem, A., Schreiber, T., Nolte, S., Zellmer, H., Tünnermann, A., et al. (2005). High-power rod-type photonic crystal fiber laser. Opt. Express *13*, 1055–1058.

Limpert, J., Hädrich, S., Rothhardt, J., Krebs, M., Eidam, T., Schreiber, T., and Tünnermann, A. (2011). Ultrafast fiber lasers for strong-field physics experiments. Laser Photon. Rev. *5*, 634–646.

Limpert, J., Klenke, A., Kienel, M., Breitkopf, S., Eidam, T., Hädrich, S., Jauregui, C., and Tünnermann, A. (2014). Performance scaling of ultrafast laser systems by coherent addition of femtosecond pulses. IEEE J. Sel. Top. Quantum Electron. *20*, 268–277.

Limpert, J., Roser, F., Klingebiel, S., Schreiber, T., Wirth, C., Peschel, T., Eberhardt, R., and Tunnermann, A. (2007). The rising power of fiber lasers and amplifiers. IEEE J. Sel. Top. Quantum Electron. *13*, 537–545.

Limpert, J., Roser, F., Schreiber, T., and Tunnermann, A. (2006). High-power ultrafast fiber laser systems. IEEE J. Sel. Top. Quantum Electron. *12*, 233–244.

Limpert, J., Schreiber, T., Clausnitzer, T., Zöllner, K., Fuchs, H.J., Kley, E.B., Zellmer, H., and Tünnermann, A. (2002). High-power femtosecond Yb-doped fiber amplifier. Opt. Express *10*, 628–638.

Limpert, J., Schreiber, T., Nolte, S., Zellmer, H., and Tünnermann, A.E.D.Q.G. (2004). All fiber chirped-pulse amplification system based on compression in air-guiding photonic bandgap fiber. Paper presented at: Advanced Solid-State Photonics (TOPS) (Santa Fe, New Mexico: Optical Society of America).

Limpert, J., Stutzki, F., Jansen, F., Otto, H.-J., Eidam, T., Jauregui, C., and Tünnermann, A. (2012). Yb-doped large-pitch fibres: effective single-mode operation based on higher-order mode delocalisation. Light Sci. Appl. *1*, e8.

Liu, C., Chang, G., Litchinitser, N., Guertin, D., Jacobsen, N., Tankala, K., and Galvanauskas, A. (2007). Chirally Coupled Core Fibers at 1550-nm and 1064-nm for Effectively Single-Mode Core Size Scaling. Paper presented at: 2007 Conference on Lasers and Electro-Optics (CLEO).

Liu, G., Jiang, X., Wang, A., Chang, G., Kaertner, F., and Zhang, Z. (2018). Robust 700 MHz mode-locked Yb:fiber laser with a biased nonlinear amplifying loop mirror. Opt. Express *26*, 26003–26008.

Liu, W., Chia, S.-H., Chung, H.-Y., Greinert, R., Kärtner, F.X., and Chang, G. (2017a). Energetic ultrafast fiber laser sources tunable in 1030–1215 nm for deep tissue multi-photon microscopy. Opt. Express *25*, 6822–6831.

Liu, W., Li, C., Zhang, Z., Kärtner, F.X., and Chang, G. (2016a). Self-phase modulation enabled, wavelength-tunable ultrafast fiber laser sources: an energy scalable approach. Opt. Express *24*, 15328–15340.

Liu, W., Liao, R., Zhao, J., Cui, J., Song, Y., Wang, C., and Hu, M. (2019). Femtosecond Mamyshev oscillator with 10-MW-level peak power. Optica *6*, 194–197.

Liu, W., Pang, L., Han, H., Tian, W., Chen, H., Lei, M., Yan, P., and Wei, Z. (2016b). 70-fs mode-locked erbium-doped fiber laser with topological insulator. Sci. Rep. *6*, 19997.

Liu, W., Schimpf, D.N., Eidam, T., Limpert, J., Tunnermann, A., Kartner, F.X., and Chang, G. (2015a). Pre-chirp managed nonlinear amplification in fibers delivering 100 W, 60 fs pulses. Opt. Lett. *40*, 151–154.

Liu, X., Svane, A.S., Lægsgaard, J., Tu, H., Boppart, S.A., and Turchinovich, D. (2015b). Progress in Cherenkov femtosecond fiber lasers. J. Phys. D Appl. Phys. *49*, 023001.

Liu, Y., Zhang, J.-G., Chen, G., Zhao, W., and Bai, J. (2010). Low-timing-jitter, stretched-pulse passively mode-locked fiber laser with tunable repetition rate and high operation stability. J. Opt. *12*, 095204.

Liu, Z., Ziegler, Z.M., Wright, L.G., and Wise, F.W. (2017b). Megawatt peak power from a Mamyshev oscillator. Optica *4*, 649–654.

Luo, D., Li, W., Liu, Y., Wang, C., Zhu, Z., Zhang, W., and Zeng, H. (2016). High-power self-similar amplification seeded by a 1 GHz harmonically mode-locked Yb-fiber laser. Appl. Phys. Express *9*, 82702.

Ma, C., Khanolkar, A., and Chong, A. (2019). High-performance tunable, self-similar fiber laser. Opt. Lett. *44*, 1234–1236.

Luo, D., Liu, Y., Gu, C., Wang, C., Zhu, Z., Zhang, W., Deng, Z., Zhou, L., Li, W., and Zeng, H. (2018). High-power Yb-fiber comb based on pre-chirped-management self-similar amplification. Appl. Phys. Lett. *112*, 61106.

Ma, D., Cai, Y., Zhou, C., Zong, W., Chen, L., and Zhang, Z. (2010). 37.4 fs pulse generation in an Er:fiber laser at a 225 MHz repetition rate. Opt. Lett. *35*, 2858–2860.

Malinowski, A., Piper, A., Price, J.H.V., Furusawa, K., Jeong, Y., Nilsson, J., and Richardson, D.J. (2004). Ultrashort-pulse Yb3+-fiber-based laser and amplifier system producing > 25-W average power. Opt. Lett. *29*, 2073–2075.

Mao, D., Liu, X., Han, D., and Lu, H. (2013). Compact all-fiber laser delivering conventional and dissipative solitons. Opt. Lett. *38*, 3190–3193.

Martinez, A., and Yamashita, S. (2011). Multi-gigahertz repetition rate passively modelocked fiber lasers using carbon nanotubes. Opt. Express *19*, 6155–6163.

Martinez, A., and Yamashita, S. (2012). 10 GHz fundamental mode fiber laser using a graphene saturable absorber. Appl. Phys. Lett. *101*, 041118.

Martinez, O. (1987). 3000 times grating compressor with positive group velocity dispersion: application to fiber compensation in 1.3-1.6 μm region. IEEE J. Quantum Electron. *23*, 59–64.

Mehravar, S., Norwood, R.A., Peyghambarian, N., and Kieu, K. (2016). Real-time dual-comb spectroscopy with a free-running bidirectionally mode-locked fiber laser. Appl. Phys. Lett. *108*, 231104.

Millot, G., Pitois, S., Yan, M., Hovhannisyan, T., Bendahmane, A., Hänsch, T.W., and Picqué, N. (2016). Frequency-agile dual-comb spectroscopy. Nat. Photon. *10*, 27–30.

Mitschke, F.M., and Mollenauer, L.F. (1986). Discovery of the soliton self-frequency shift. Opt. Lett. *11*, 659–661.

Mueller, M., Aleshire, C., Stark, H., Buldt, J., Steinkopff, A., Klenke, A., Tünnermann, A., and Limpert, J. (2020). 10.4 kW coherently-combined ultrafast fiber laser. Paper presented at: ProcSPIE.

Muller, M., Kienel, M., Klenke, A., Gottschall, T., Shestaev, E., Plotner, M., Limpert, J., and Tunnermann, A. (2016). 1 kW 1 mJ eight-channel ultrafast fiber laser. Opt. Lett. *41*, 3439–3442.

Muller, M., Klenke, A., Steinkopff, A., Stark, H., Tunnermann, A., and Limpert, J. (2018). 3.5 kW coherently combined ultrafast fiber laser. Opt. Lett. *43*, 6037–6040.

Nakajima, Y., Hata, Y., and Minoshima, K. (2019). All-polarization-maintaining, polarization-multiplexed, dual-comb fiber laser with a nonlinear amplifying loop mirror. Opt. Express *27*, 14648–14656.

Nakazawa, M., Kimura, Y., and Suzuki, K. (1989). Soliton amplification and transmission with Er3+-doped fibre repeater pumped by GaInAsP laser diode. Electronics Letters *25*, 199–200.

Nicholson, J.W., Yablon, A.D., Westbrook, P.S., Feder, K.S., and Yan, M.F. (2004). High power, single mode, all-fiber source of femtosecond pulses at 1550 nm and its use in supercontinuum generation. Opt. Express *12*, 3025–3034.

Nilsson, J., and Payne, D.N. (2011). High-power fiber lasers. Science *332*, 921–922.

Nilsson, J., Sahu, J.K., Jeong, Y., Clarkson, W.A., Selvas, R., Grudinin, A.B., and Alam, S. (2003). High-power fiber lasers: new developments. Paper presented at: Advances in Fiber Lasers.

Nitta, K., Jie, C., Mizuguchi, T., Hu, G., Zheng, Z., and Yasui, T. (2018). Dual-comb spectroscopy in THz region using a single free-running dual-wavelength mode-locked fiber laser*10826* (SPIE).

Niu, F., Li, J., Yang, W., Zhang, Z., and Wang, A. (2018). Fiber-based high-energy femtosecond pulses tunable from 920 to 1030 nm for two-photon microscopy. IEEE Photon. Technol. Lett. *30*, 1479–1482.

Nyushkov, B., Kobtsev, S., Antropov, A., Kolker, D., and Pivtsov, V. (2019). Femtosecond 78-nm tunable Er:fibre laser based on drop-shaped resonator topology. J. Lightwave Technol. *37*, 1359–1363.

Ogino, J., Sueda, K., Kurita, T., Kawashima, T., and Miyanaga, N. (2013). Development of high-energy fiber CPA system. EPJ Web of Conferences 59.

Okhotnikov, O., Grudinin, A., and Pessa, M. (2004). Ultra-fast fibre laser systems based on

SESAM technology: new horizons and applications. New J. Phys. *6*, 177.

Oktem, B., Ülgüdür, C., and Ilday, F.Ö. (2010). Soliton–similariton fibre laser. Nat. Photon. *4*, 307–311.

Olson, J., Ou, Y.H., Azarm, A., and Kieu, K. (2018). Bi-directional mode-locked thulium fiber laser as a single-cavity dual-comb source. IEEE Photon. Technol. Lett. *30*, 1772–1775.

Ozeki, Y., Takushima, Y., Aiso, K., and Kikuchi, K. (2005). High repetition-rate similariton generation in normal dispersion erbium-doped fiber amplifiers and its application to multi-wavelength light sources. IEICE Trans. *88-C*, 904–911.

Ozeki, Y., Takushima, Y., Aiso, K., Taira, K., and Kikuchi, K. (2004). Generation of 10 GHz similariton pulse trains from 1.2 km-long erbium-doped fibre amplifier for application to multi-wavelength pulse sources. Electronics Letters *40*, 1103–1104.

Papadopoulos, D.N., Zaouter, Y., Hanna, M., Druon, F., Mottay, E., Cormier, E., and Georges, P. (2007). Generation of 63 fs 4.1 MW peak power pulses from a parabolic fiber amplifier operated beyond the gain bandwidth limit. Opt. Lett. *32*, 2520–2522.

Paschotta, R., Nilsson, J., Tropper, A.C., and Hanna, D.C. (1997). Ytterbium-doped fiber amplifiers. IEEE J. Quantum Electron. *33*, 1049–1056.

Pawliszewska, M., Dużyńska, A., Zdrojek, M., and Sotor, J. (2020). Wavelength- and dispersion-tunable ultrafast holmium-doped fiber laser with dual-color operation. Opt. Lett. *45*, 956–959.

Plotner, M., Bock, V., Schultze, T., Beier, F., Schreiber, T., Eberhardt, R., and Tunnermann, A. (2017). High power sub-ps pulse generation by compression of a frequency comb obtained by a nonlinear broadened two colored seed. Opt. Express *25*, 16476–16483.

Regelskis, K., Želudevičius, J., Viskontas, K., and Račiukaitis, G. (2015). Ytterbium-doped fiber ultrashort pulse generator based on self-phase modulation and alternating spectral filtering. Opt. Lett. *40*, 5255–5258.

Richardson, D.J., Nilsson, J., and Clarkson, W.A. (2010). High power fiber lasers: current status and future perspectives. J. Opt. Soc. Am. B *27*, B63–B92.

Rishøj, L., Tai, B., Kristensen, P., and Ramachandran, S. (2019). Soliton self-mode conversion: revisiting Raman scattering of ultrashort pulses. Optica *6*, 304–308.

Roser, F., Eidam, T., Rothhardt, J., Schmidt, O., Schimpf, D.N., Limpert, J., and Tunnermann, A. (2007). Millijoule pulse energy high repetition rate femtosecond fiber chirped-pulse amplification system. Opt. Lett. *32*, 3495–3497.

Röser, F., Schimpf, D., Schmidt, O., Ortac, B., Rademaker, K., Limpert, J., and Tünnermann, A. (2007). 90-W average-power, high-energy femtosecond fiber laser system. Fiber Lasers IV: Technology, Systems, and Applications, *6453* (Proc. SPIE).

Set, S.Y., Yaguchi, H., Tanaka, Y., and Jablonski, M. (2004). Laser mode locking using a saturable absorber incorporating carbon nanotubes. J. Lightwave Technol. *22*, 51.

Shah, L., Liu, Z., Hartl, I., Imeshev, G., Cho, G.C., and Fermann, M.E. (2005). High energy femtosecond Yb cubicon fiber amplifier. Opt. Express *13*, 4717–4722.

Shi, H., Song, Y., Li, T., Wang, C., Zhao, X., Zheng, Z., and Hu, M. (2018). Timing jitter of the dual-comb mode-locked laser: a quantum origin and the ultimate effect on high-speed time- and frequency-domain metrology. IEEE J. Sel. Top. Quantum Electron. *24*, 1–10.

Shi, W., Fang, Q., Zhu, X.S., Norwood, R.A., and Peyghambarian, N. (2014). Fiber lasers and their applications [Invited]. Appl. Opt. *53*, 6554–6568.

Sidorenko, P., Fu, W., and Wise, F. (2019). Nonlinear ultrafast fiber amplifiers beyond the gain-narrowing limit. Optica *6*.

Sidorenko, P., Fu, W., Wright, L.G., Olivier, M., and Wise, F.W. (2018). Self-seeded, multi-megawatt, Mamyshev oscillator. Opt. Lett. *43*, 2672–2675.

Smith, A.V., and Smith, J.J. (2011). Mode instability in high power fiber amplifiers. Opt. Express *19*, 10180–10192.

Snitzer, E., Po, H., Hakimi, F., Tumminelli, R., and McCollum, B.C. (1988). DOUBLE CLAD, OFFSET CORE Nd FIBER LASER. Paper presented at: Optical Fiber Sensors (New Orleans, Louisiana: Optical Society of America).

Soh, D.B., Nilsson, J., and Grudinin, A.B. (2006a). Efficient femtosecond pulse generation using a parabolic amplifier combined with a pulse compressor. I. Stimulated Raman-scattering effects. J. Opt. Soc. Am. B *23*, 1–9.

Soh, D.B., Nilsson, J., and Grudinin, A.B. (2006b). Efficient femtosecond pulse generation using a parabolic amplifier combined with a pulse compressor. II. Finite gain-bandwidth effect. J. Opt. Soc. Am. B *23*, 10–19.

Song, H., Liu, B., Li, Y., Song, Y., He, H., Chai, L., Hu, M., and Wang, C. (2017). Practical 24-fs, 1-μJ, 1-MHz Yb-fiber laser amplification system. Opt. Express *25*, 7559–7566.

Song, J., Hu, X., Wang, H., Zhang, T., Wang, Y., Liu, Y., and Zhang, J. (2019a). All-polarization-maintaining, semiconductor saturable absorbing mirror mode-locked femtosecond Er-doped fiber laser with a gigahertz fundamental repetition rate. Laser Phys. Lett. *16*, 095102.

Song, J., Wang, H., Huang, X., Hu, X., Zhang, T., Wang, Y., Liu, Y., and Zhang, J. (2019b). Compact low-noise passively mode-locked Er-doped femtosecond all-fiber laser with 268 GHz fundamental repetition rate. Appl. Opt. *58*, 1733–1738.

Stark, H., Buldt, J., Muller, M., Klenke, A., Tunnermann, A., and Limpert, J. (2019). 23 mJ high-power fiber CPA system using electro-optically controlled divided-pulse amplification. Opt. Lett. *44*, 5529–5532.

Stock, M., Galvanauskas, A., Fermann, M., Mourou, G., and Harter, D. (1993). Generation of high-power femtosecond optical pulses by chirped pulse amplification in erbium doped fibers. Paper presented at: Proc Opt Soc Am Top Meeting on Nonlinear Guided Wave Phenomena.

Strickland, D., and Mourou, G. (1985). Compression of amplified chirped optical pulses. Opt. Commun. *55*, 447–449.

Stutzki, F., Jansen, F., Eidam, T., Steinmetz, A., Jauregui, C., Limpert, J., and Tünnermann, A. (2011). High average power large-pitch fiber amplifier with robust single-mode operation. Opt. Lett. *36*, 689–691.

Suh, M.-G., Yang, Q.-F., Yang, K.Y., Yi, X., and Vahala, K.J. (2016). Microresonator soliton dual-comb spectroscopy. Science *354*, 600.

Suzuki, K., Kimura, Y., and Nakazawa, M. (1989). Subpicosecond soliton amplification and transmission using Er3+-doped fibers pumped by InGaAsP laser diodes. Opt. Lett. *14*, 865–867.

Takayanagi, J., Sugiura, T., Yoshida, M., and Nishizawa, N. (2006). 1.0-1.7-μm wavelength-tunable ultrashort-pulse generation using femtosecond Yb-doped fiber laser and photonic crystal fiber. IEEE Photon. Technol. Lett. *18*, 2284–2286.

Tamura, K., and Nakazawa, M. (1996). Pulse compression by nonlinear pulse evolution with reduced optical wave breaking in erbium-doped fiber amplifiers. Opt. Lett. *21*, 68–70.

Tauser, F., Adler, F., and Leitenstorfer, A. (2004). Widely tunable sub-30-fs pulses from a compact erbium-doped fiber source. Opt. Lett. *29*, 516–518.

Taylor, J.R. (2016). Tutorial on fiber-based sources for biophotonic applications. J. Biomed. Opt. *21*, 61010.

Tomlinson, W.J., Stolen, R.H., and Johnson, A.M. (1985). Optical wave breaking of pulses in nonlinear optical fibers. Opt. Lett. *10*, 457–459.

Townes, C.H. (2002). How the Laser Happened: Adventures of a Scientist (Oxford University Press).

Treacy, E. (1969). Optical pulse compression with diffraction gratings. IEEE J. Quantum Electron. *5*, 454–458.

Tu, H., and Boppart, S.A. (2013). Coherent fiber supercontinuum for biophotonics. Laser Photon. Rev. *7*, 628–645.

Tu, H., Laegsgaard, J., Zhang, R., Tong, S., Liu, Y., and Boppart, S.A. (2013). Bright broadband coherent fiber sources emitting strongly blue-shifted resonant dispersive wave pulses. Opt. Express *21*, 23188–23196.

Tunnermann, A., Schreiber, T., and Limpert, J. (2010). Fiber lasers and amplifiers: an ultrafast performance evolution. Appl. Opt. *49*, F71–F78.

Tunnermann, A., Schreiber, T., Roser, F., Liem, A., Hofer, S., Zellmer, H., Nolte, S., and Limpert, J. (2005). The renaissance and bright future of fibre lasers. J. Phys. B At. Mol. Opt. Phys. *38*, S681–S693.

van Howe, J., Lee, J.H., Zhou, S., Wise, F., Xu, C., Ramachandran, S., Ghalmi, S., and Yan, M.F.

(2007). Demonstration of soliton self-frequency shift below 1300 nm in higher-order mode, solid silica-based fiber. Opt. Lett. *32*, 340–342.

Villares, G., Hugi, A., Blaser, S., and Faist, J. (2014). Dual-comb spectroscopy based on quantum-cascade-laser frequency combs. Nat. Commun. *5*, 5192.

Wai, P.K.A., Menyuk, C.R., Lee, Y.C., and Chen, H.H. (1986). Nonlinear pulse propagation in the neighborhood of the zero-dispersion wavelength of monomode optical fibers. Opt. Lett. *11*, 464–466.

Wan, P., Yang, L.M., and Liu, J. (2013). All fiber-based Yb-doped high energy, high power femtosecond fiber lasers. Opt. Express *21*, 29854–29859.

Wang, A., Yang, H., and Zhang, Z. (2011). 503MHz repetition rate femtosecond Yb: fiber ring laser with an integrated WDM collimator. Opt. Express *19*, 25412–25417.

Wang, H.-Y., Huang, S.-W., Li, D.-R., Lin, B.-S., and Chan, M.-C. (2015). Nonlinear light microscopy by a 1.2-μm fiber-laser-based femtosecond dispersive wave source. IEEE Photon. J. *7*, 1–8.

Wang, W., Lin, W., Cheng, H., Zhou, Y., Qiao, T., Liu, Y., Ma, P., Zhou, S., and Yang, Z. (2019). Gain-guided soliton: scaling repetition rate of passively modelocked Yb-doped fiber lasers to 12.5 GHz. Opt. Express *27*, 10438–10448.

Wang, Y., Li, J., Zhai, B., Hu, Y., Mo, K., Lu, R., and Liu, Y. (2016). Tunable and switchable dual-wavelength mode-locked Tm3+-doped fiber laser based on a fiber taper. Opt. Express *24*, 15299–15306.

Ward, B., Robin, C., and Dajani, I. (2012). Origin of thermal modal instabilities in large mode area fiber amplifiers. Opt. Express *20*, 11407–11422.

Washburn, B.R., Fox, R.W., Newbury, N.R., Nicholson, J.W., Feder, K., Westbrook, P.S., and Jørgensen, C.G. (2004). Fiber-laser-based frequency comb with a tunable repetition rate. Opt. Express *12*, 4999–5004.

Wigley, P.G.J., French, P.M.W., and Taylor, J.R. (1990). Mode-locking of a continuous wave neodymium doped fiber laser with a linear external cavity. Electronics Letters *26*, 1238–1240.

Wise, F.W., Chong, A., and Renninger, W.H. (2008). High-energy femtosecond fiber lasers based on pulse propagation at normal dispersion. Laser Photon. Rev. *2*, 58–73.

Woodward, I.R., and Kelleher, J.R.E. (2015). 2D saturable absorbers for fibre lasers. Appl. Sci. *5*, 1440–1456.

Wu, K., Zhang, X., Wang, J., and Chen, J. (2015a). 463-MHz fundamental mode-locked fiber laser based on few-layer MoS(2) saturable absorber. Opt. Lett. *40*, 1374–1377.

Wu, X., Yang, L., Zhang, H., Yang, H., Wei, H., and Li, Y. (2015b). Hybrid mode-locked Er-fiber oscillator with a wide repetition rate stabilization range. Appl. Opt. *54*, 1681–1687.

Xing, L., Weiwen, Z., Guang, Y., and Jianping, C. (2015). Direct generation of 148 nm and 44.6 fs pulses in an erbium-doped fiber laser. IEEE Photon. Technol. Lett. *27*, 93–96.

Xu, C., and Wise, F.W. (2013). Recent advances in fiber lasers for nonlinear microscopy. Nat. Photon. *7*, 875–882.

Yang, H., Wang, A., and Zhang, Z. (2012). Efficient femtosecond pulse generation in an all-normal-dispersion Yb:fiber ring laser at 605 MHz repetition rate. Opt. Lett. *37*, 954–956.

Yang, H., Wu, X., Zhang, H., Zhao, S., Yang, L., Wei, H., and Li, Y. (2016). Optically stabilized Erbium fiber frequency comb with hybrid mode-locking and a broad tunable range of repetition rate. Appl. Opt. *55*, D29–D34.

Yang, K., Jiang, J., Guo, Z., Hao, Q., and Zeng, H. (2018). Tunable femtosecond laser from 965 to 1025 nm in fiber optical parametric oscillator. IEEE Photon. Technol. Lett. *30*, 607–610.

Yao, Y., Agrawal, G.P., and Knox, W.H. (2015). Yb:fiber laser-based, spectrally coherent and efficient generation of femtosecond 1.3-μm pulses from a fiber with two zero-dispersion wavelengths. Opt. Lett. *40*, 3631–3634.

Yu, H., Wang, X., Zhang, H., Su, R., Zhou, P., and Chen, J. (2016). Linearly-polarized fiber-integrated nonlinear CPA system for high-average-power femtosecond pulses generation at 1.06 μm. J. Lightwave Technol. *34*, 4271–4277.

Yu, M., Okawachi, Y., Griffith, A.G., Picqué, N., Lipson, M., and Gaeta, A.L. (2018a). Silicon-chip-based mid-infrared dual-comb spectroscopy. Nat. Commun. *9*, 1869.

Wu, T.-H., Carlson, D.R., and Jones, R. (2013). A high-power fiber laser system for dual-comb spectroscopy in the vacuum-ultraviolet. Paper presented at: Frontiers in Optics (Orlando, Florida: Optical Society of America).

Yu, Y., Fang, S., Teng, H., Zhu, J., Chang, G., and Wei, Z. (2019). 1-MHz, energetic ultrafast source tunable between 940-1250 nm for multi-photon microscopy. Paper presented at: Conference on Lasers and Electro-Optics (San Jose, California: Optical Society of America).

Yu, Y., Teng, H., Wang, H., Wang, L., Zhu, J., Fang, S., Chang, G., Wang, J., and Wei, Z. (2018b). Highly-stable mode-locked PM Yb-fiber laser with 10 nJ in 93-fs at 6 MHz using NALM. Opt. Express *26*, 10428–10434.

Yun, L., Liu, X., and Mao, D. (2012). Observation of dual-wavelength dissipative solitons in a figure-eight erbium-doped fiber laser. Opt. Express *20*, 20992–20997.

Zaouter, Y., Papadopoulos, D.N., Hanna, M., Boullet, J., Huang, L., Aguergaray, C., Druon, F., Mottay, E., Georges, P., and Cormier, E. (2008). Stretcher-free high energy nonlinear amplification of femtosecond pulses in rod-type fibers. Opt. Lett. *33*, 107–109.

Zaouter, Y., Papadopoulos, D.N., Hanna, M., Druon, F., Cormier, E., and Georges, P. (2007). Third-order spectral phase compensation in parabolic pulse compression. Opt. Express *15*, 9372–9377.

Zervas, M.N. (2014). High power ytterbium-doped fiber lasers — fundamentals and applications. Int. J. Mod. Phys. B *28*, 1442009.

Zervas, M.N., and Codemard, C.A. (2014). High power fiber lasers: a review. IEEE J. Sel. Top. Quantum Electron. *20*, 219–241.

Zhang, J., Kong, Z., Liu, Y., Wang, A., and Zhang, Z. (2016). Compact 517 MHz soliton mode-locked Er-doped fiber ring laser. Photon. Res. *4*, 27–29.

Zhao, J., Li, W., Wang, C., Liu, Y., and Zeng, H. (2014). Pre-chirping management of a self-similar Yb-fiber amplifier towards 80 W average power with sub-40 fs pulse generation. Opt. Express *22*, 32214–32219.

Zhao, K., Jia, H., Wang, P., Guo, J., Xiao, X., and Yang, C. (2019). Free-running dual-comb fiber laser mode-locked by nonlinear multimode interference. Opt. Lett. *44*, 4323–4326.

Zhao, X., Hu, G., Zhao, B., Li, C., Pan, Y., Liu, Y., Yasui, T., and Zheng, Z. (2016). Picometer-resolution dual-comb spectroscopy with a free-running fiber laser. Opt. Express *24*, 21833–21845.

Zhao, X., Zheng, Z., Liu, L., Liu, Y., Jiang, Y., Yang, X., and Zhu, J. (2011). Switchable, dual-wavelength passively mode-locked ultrafast fiber laser based on a single-wall carbon nanotube modelocker and intracavity loss tuning. Opt. Express *19*, 1168–1173.

Zhao, X., Zheng, Z., Liu, L., Wang, Q., Chen, H., and Liu, J. (2012a). Fast, long-scan-range pump-probe measurement based on asynchronous sampling using a dual-wavelength mode-locked fiber laser. Opt. Express *20*, 25584–25589.

Zhao, Z., Dunham, B.M., Bazarov, I., and Wise, F.W. (2012b). Generation of 110 W infrared and 65 W green power from a 1.3-GHz sub-picosecond fiber amplifier. Opt. Express *20*, 4850–4855.

Zhao, Z., and Kobayashi, Y. (2016). Ytterbium fiber-based, 270 fs, 100 W chirped pulse amplification laser system with 1 MHz repetition rate. Appl. Phys. Express *9*, 12701.

Zhou, S., Kuznetsova, L., Chong, A., and Wise, F.W. (2005). Compensation of nonlinear phase shifts with third-order dispersion in short-pulse fiber amplifiers. Opt. Express *13*, 4869–4877.

Zhou, S., Wise, F.W., and Ouzounov, D.G. (2007). Divided-pulse amplification of ultrashort pulses. Opt. Lett. *32*, 871–873.

Zhou, Y., Cheung, K.K.Y., Yang, S., Chui, P.C., and Wong, K.K.Y. (2009). Widely tunable picosecond optical parametric oscillator using highly nonlinear fiber. Opt. Lett. *34*, 989–991.

Zhu, X.S., Zhu, G.W., Wei, C., Kotov, L.V., Wang, J.F., Tong, M.H., Norwood, R.A., and Peyghambarian, N. (2017). Pulsed fluoride fiber lasers at 3 mu m [Invited]. J. Opt. Soc. Am. B *34*, A15–A28.